Generation of a model for the description of the viscosity of bio-oil produced by fast pyrolysis of wheat straw

Muhammad Rizwan Younis

Thesis to obtain the Master of Science degree in Energy Engineering and Management (MEGE)

Energy Technology (ENTECH)

Supervisors:

Prof. Dr.-Ing. Jörg Sauer

Prof. Francisco Manuel da Silva Lemos

Examination committee:

Chairperson: Prof. José Alberto Caiado Falcão de Campos

Supervisors: Prof. Francisco Manuel da Silva Lemos

Member of the Committee: Prof. João Manuel Nunes Alvarinhas Fareleira

November 2014

Acknowledgements

First of all I would like to sincerely thank my supervisors Prof. Dr.-Ing. Jörg Sauer and Prof Francisco Manuel da Silva Lemos, for their guidance and encouragement during my research work. Their academic advice, patience, understanding and support have helped me during the completion of this thesis. He has always been a source of inspiration, a mentor and great teacher for me.

I would like to thank my advisor Dr.Axel Funke for his support and advice. He helped me in every nick of time and motivates me. I am very grateful to him for helping me throughout the Master thesis. He has supported me in every possible way and his help eventually lead to the completion of this Master thesis.

Furthermore I would like to thank Dr. Klaus Raffelt for his guidance and support throughout the completion of this thesis.

I wish to express my gratitude to the analytic group of Pia Griessheimer and her laboratory assistants Kathrin Biro, Jessica Maier, Anthea Guiditta and Eva Eger.

At the end I would like to thank my parents for their continuous support and encouragement**.** My special thanks to my colleagues who always stood by me in difficult time.

Abstract

Bio-oil is a major product of biomass fast pyrolysis that could potentially be used in motor engines, boilers, furnaces and turbines for heat and power. However bio-oil of bioliq® is not intended for direct use in motor engines. It will be gasified to produce synthesis gas. Bioliq® Process analytics provides bio-oil characterization and rheological characterization is a key process parameter in this analysis. The aim of this work is to evaluate the role of viscosity of organic condensate obtained from wheat straw for the technical feasibility of the organic condensate cycle. This has to be done by means of a model that is able to adequately describe the viscosity as a function of relevant process parameters. The developed model of temperature is helpful to investigate the drop of heat transfer in the heat exchangers of the organic condensate cycle when glycol is replaced by an organic condensate. Viscosity-temperature profile follows an Arrhenius-type-relationship, where the viscosity of the bio-oil decreases exponentially with increasing temperature. As solid content increases, exponential increase of viscosity takes place. By increasing water content, decrease of viscosity takes place on logarithmic scale. Investigation of drop of heat transfer in heat exchanger shows that Nusselt number decreases with the increase of viscosity. Overall, from this study, it can be concluded that viscosity is influenced by the key parameters determining the organic condensate cycle through intrinsic relationships.

Key words: Rheology, temperature, solid content, water content, Nusselt number

Resumo

Bio-óleo é um dos produtos principais de pirólise rápida de biomassa que potencialmente terá utilização em motores, caldeiras e turbinas para a produção de calor e eletricidade. No entanto bio-óleo produzido pelo processo bioliq® não se destina a ser diretamente utilizado em motores. A sua utilização implicará a sua gasificação para produzir gás de síntese. Os dados analíticos obtidos no processo Bioliq® fornecem uma caracterização de composição e reologia do bio-óleo que são parâmetros chave nesta análise. O objetivo deste trabalho é avaliar o papel da viscosidade na viabilidade do ciclo de condensados orgânicos. Esta análise tem de ser feita recorrendo a um modelo que seja capaz de descrever adequadamente a viscosidade em função dos parâmetros de processo mais relevantes. O modelo que foi desenvolvido para a temperatura é útil para investigar a quebra de quantidade de calor transferido nos permutadores de calor do ciclo de condensados orgânicos quando o glicol é substituído por um condensado orgânico. Os perfis de viscosidade-temperatura seguem uma relação do tipo de Arrhenius, onde a viscosidade do bio-óleo diminui exponencialmente com o aumento de temperatura. À medida que o teor de sólidos aumenta ocorre um aumento exponencial na viscosidade. O aumento do teor de água diminui a viscosidade de forma logarítmica. O estudo da transferência de calor no permutador de calor mostra que o número de Nusselt diminui com o aumento da viscosidade. De forma geral, deste estudo podemos concluir que a viscosidade é influenciada pelos parâmetros chave que determinam a composição do condensado orgânico.

Palavras-chave: Reologia, temperatura, teor de sólidos, teor de água, número de Nusselt

List of Symbols and Units

Symbols/ Description	Unit
Energy	J=joule or PJ= Peta joules
Energy density	GJ/m^3
Distance or radius	Km
Area	m^2 or ha
Length	m
Pressure	Bar or kPa
Temperature	^0C
Mass	kg
Density	kg/m^3
Heating values	MJ/kg
Flow rate	m^3/min
Heating rate	°C/s
Heat transfer rate	W/m^2
Surface tension	N/m
Drag force	N
Dynamic viscosity	Pa.s
Gas constant	J/mol/K=8314 (J/mol/K)
Shear rate $\dot{\gamma}$	S^{-1}
Activation energy E_a	J/mol
a= Thermal diffusivity	m^2/s
k= Thermal conductivity	W/ (m*K)
C_p= Specific heat	J/ (Kg*K)

Molecular formula	Description
CO_2	Carbon dioxide
$C_6H_9O_4$	Lignocellulose condensate
C_2H	Rough empirical formula of char
$C_3H_5O_2$	Pyrolysis tar
H_2O	Water
CHO	Non-condensable gases
$C_5H_8O_3$	Biosyncrude®
CO	Carbon mono-oxide
CH_4	Methane
H_2	Hydrogen
HCl	Hydrochloric acid
H_2S	Hydrogen disulphide
NH_3	Ammonia
HCN	Hydrogen cyanide
$CO+H_2$	Syngas

Abbreviations

Abbreviations,	Description
BtL	Biomass-to-liquid
BTL2	Biomass to liquid in two steps
LPG	Liquid petroleum gas
CNG	Compressed natural gas
KIT	Karlsruhe Institute for Technology
TSM	Twin screw mixer
IGCC	Integrated gasification combined cycle power plants
CHP	Combined heat and power plants
DME	Dimethylether
Wt. %	Percentage by weight
H/C	Hydrogen to carbon ratio
m .%	Percentage by mass
HHV	Higher heating value
LHV	Lower heating value
GC-MSD	Gas chromatography-mass selective detector
FP	Fast pyrolysis
WIS	Water-insoluble
H.E	Heat exchanger
Re	Reynold number
Pr	Prandtl number
Nu	Nusselt number
q_{lost}	Heat loss
q_{gain}	Heat gain
A_i	Inside tube area
U_i	Overall heat transfer coefficient based on inside area
ΔT_{lm}	Logarithmic mean temperature difference
v	Kinematic viscosity
μ or η	Dynamic viscosity
ϭ	Greek letter sigma i.e stress
μ_a	Apparent viscosity
$\dot{\gamma}$	Velocity gradient or shear rate
a	Pre-exponential factor
R	Gas constant

Contents

List of Figures:

List of Tables:

Chapter 1: Introduction

1.1 Motivation:

Energy plays important role in every aspect of life. Society is in a constant struggle to find adequate sources to meet the growing energy demands because of industrial and economic growth. Man has been dependent upon fossil fuels like coal and oil as his primary source of energy for a few decades. These fuels have been on earth for hundreds and thousands of years. Fossil fuels are non-renewable resources and are being depleted. Therefore, these resources cannot be considered as an eternal resource of energy. Therefore, it is now time to discover alternative renewable energy resources for the future [1].

The world energy consumption is on the rise because of the rapid population growth and the gradual improvement of living standards in the developing countries in comparison to the industrialized countries. Figure 1.1 shows that in 2011 total primary energy supply is around **$5.44*10^{11}$J** per year. About 80 % of the energy is supplied through fossil fuels. Biomass contributes about 10%. The energy mix shows the dominance of fossil fuels especially oil as compared to the slow and continuously growing quantities of renewable energies [2].

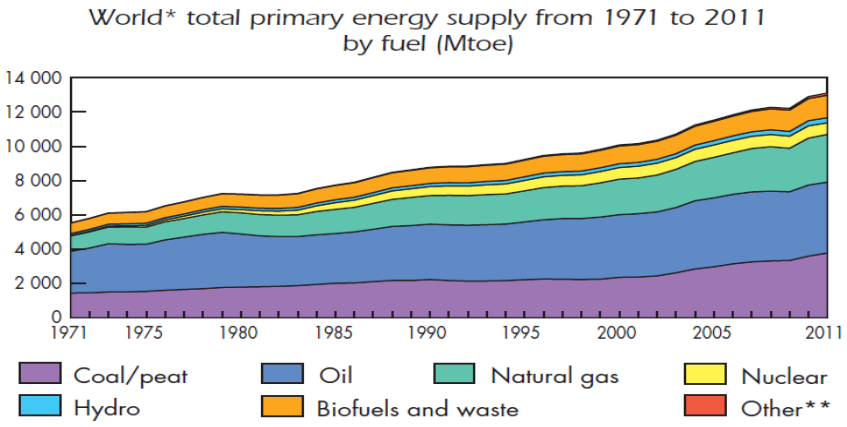

Figure 1.1: World total primary energy supply from 1971 to 2009 by fuel (Gtoe) [2]

With current consumption trends, world energy demand is estimated to grow by 50% between 2005 and 2030. The two largest energy consumption rise contributors are transport and the industry sector. Traditional liquid fuels developed from fossil resources such as diesel, gasoline, and liquefied petroleum gas (LPG) and compressed natural gas (CNG), play a valuable role in the transportation sector [3]. Currently, more than 90% of the energy used for transportation is derived from petroleum fuels. However, fossil fuels are being depleted. The cost of these fuels is expected to rise and these fuels emit a huge amount of greenhouse gases. One of these gases is CO_2, a major contributor to global warming.

In order to meet rising energy demands, new energy resources like solar, hydro, wind, geothermal and biomass, need to be exploited. Bio-energy has been explored as a viable solution for energy crisis in Germany and around the world. The consumption of wood and straw materials, as a source of bio-energy, in Germany has increased steadily over the past two decades. According to Germany, potential of energy from biomass is approximately 550 PJ [4]. The first generation bio-fuels, like bio-ethanol from sugar containing plants, can be used as a replacement of gasoline and bio-diesel [5]. However, the cost of these biofuels is high due to the limited raw material resource. Furthermore, fuel vs. food develops a risk of diverting crop farmland for producing liquid bio-fuels which produce negative effects to the world wide food supplies [6]. Thus, scientists and industries have begun research on alternative sources for fuel production to make fuels comparable in terms of cost and efficiency to fossil fuels and to reduce the fuel vs. food problems [7].

Looking forward to these challenges, Karlsruhe Institute for Technology (KIT) is working on bioliq® process. The primary goal of this biomass-to-liquid (BtL) research is to partly replace crude oil based hydrocarbon resources with cost-effective low quality residual biomass fuels.

The Karlsruhe bioliq® process consists of several sub-processes that are currently being implemented as separate projects, and will be presented in more detail in the next session. Briefly, the lignocellulose biomass is first liquefied by fast pyrolysis in regional plants to produce an energy-dense intermediate, composed of a viscous bio-oil and a high energy char powder. Then these products are mixed in appropriate ratio to prepare bio slurry also known as bio-syncrude®. This allows achievement of high energy density and therefore biosyncrude® is better suited to be transported to the central treatment plant. The biosyncrude® is stored and slowly stirred in tanks to avoid sedimentation of char particles. After stirring, the biosyncrude® is converted into raw syngas through an entrained flow gasifier. This raw syngas is then converted to synfuels or platform chemicals by catalysis as shown in figure 1.2.

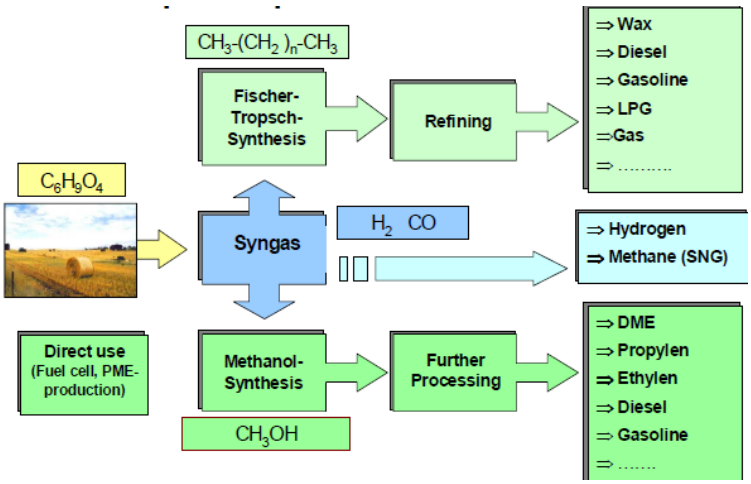

Figure 1.2: Chemical pathway to synthetic products [8]

The bio-slurry, which is obtained by the mixing of the pyrolysis products, has a volumetric energy density of about 20 $\mathbf{GJ/m^3}$ and is transported, as a high energy intermediate product, economically over long distances. For comparison: The energy density of the charge material is, for example, in the case of straw bales, is about 2 $\mathbf{GJ/m^3}$and for diesel 36$\mathbf{GJ/m^3}$. As the slurry is energy dense product of fast pyrolysis plant, the decentralized fast pyrolysis plants can be located within an economic radius of 250 km around the centrally constructed entrained-flow gasifier [8].

1.2 Objectives of work:

The bioliq® concept developed by KIT is a three step conversion process for the production of 2nd generation drop-in biofuels from biomass waste such as e.g. wheat straw. First, biomass is converted by fast pyrolysis to yield energy dense biosyncrude, a mixture of bio-oil and char. This slurry is the feed for subsequent pressurized entrained flow gasification at 8 MPa to yield producer gas free of tars. The gas is finally converted by Fischer-Tropsch synthesis to yield designer fuels. The given task is set in the first step, fast pyrolysis. This initial conversion is performed in a twin-screw mixing reactor at 500 °C. The comminuted biomass feed is thermo-chemically converted to hot pyrolysis vapors, gas, and char fines within seconds. Solid particles are separated by cyclones prior to a two-step condensation of the vapors to yield an organic and an aqueous condensate as shown in figure 1.3. The organic condensate is recycled, cooled down and used for quenching the incoming hot vapors in order to assure rapid cooling. The technical feasibility of the organic condensate has not been evaluated yet. One major aspect of the technical feasibility is the viscosity of the organic condensate because viscosity is an important parameter for the determination of pipeline size and the power required to pump fluids through it. Viscosity also plays important role in heat-exchanger and separation equipment sizing, and is a critical parameter for the efficiency of reservoir oils. It is a function of several process parameters like quenching temperature, fluid temperature, residence time/age, water and solids content. The dependency of the viscosity of the organic condensate on these parameters is generally known: with rising temperature there is a decrease in viscosity following the Arrhenius law, with increasing water content viscosity decreases, and the higher the solids content the higher the viscosity. Unknown is the quantification of these dependencies, i.e. the development of a model.

Mainly there are two major tasks:

1). To evaluate the role of viscosity for the technical feasibility of the organic condensate cycle by means of a model that is able to adequately describe the viscosity as a function of relevant process parameters. The model is to be based on experimental measurements, which have been performed on rheometer in KIT Germany. So, the purpose of this work is to characterize firstly the viscosity of organic condensate by varying fluid temperature, water content and solid content.

2). Secondly, the purpose of this study is related to heat exchanger of bioliq® plant. It was observed that during operation of the bioliq® pilot plant, the heat transfer in the heat exchangers of the organic condensate cycle dropped constantly when glycol was replaced by organic condensate. Glycol is used as preliminary material during start up of the plant and has a different viscosity than the organic condensate. It should be investigated how efficiently the observed drop in heat transfer can be explained quantitatively by the change in viscosity. If necessary, temperature correction can be performed on the basis of the developed tar model.

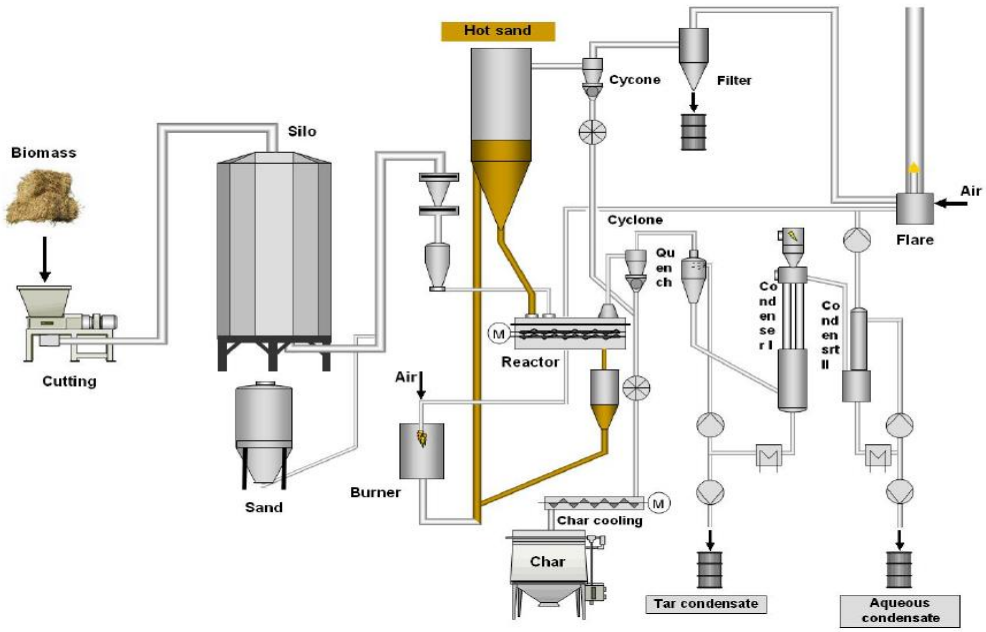

Figure 1.3: Overall plant view [10]

1.3 Structure of thesis:

This thesis is structured as follows:

Chapter 2: The Karlsruhe bioliq®- Process

This chapter represents the bioliq® process developed in Karlsruhe Institute of Technology step by step.

Chapter 3: Literature Review:

This chapter describes the previous studies on viscosity of bio-oil, viscosity measuring methods and Impacts/Effects of different parameters on viscosity. This chapter also describes theoretical study of heat exchanger and some basics of shell and tube heat exchanger which is a part of Master thesis.

Chapter 4: Methodology

This chapter presents the experimental set-up, material properties and preparation of a model for the characterization of viscosity of bio-oil produced by fast pyrolysis of wheat straw, and the experimental strategy, procedure, methods and technique used in this study.

Chapter 5: Results

This chapter shows the results achieved by the experiments mentioned in the previous chapter.

Chapter 6: Conclusions and Recommendations

This chapter summarizes the findings and presents the conclusion derived from this study. Recommendations are made for future studies.

Chapter 2: The Karlsruhe bioliq®- Process

In this chapter, the bioliq® process which is developed at KIT is illustrated. The purpose of the process is the liquid fuel synthesis from low quality biomass such as organic waste, straw or wood residues. The biosyncrude® based bioliq® process consists of sub-processes that are currently being implemented as separate projects at KIT. The two step process is simply illustrated in figure 2.1 [10].

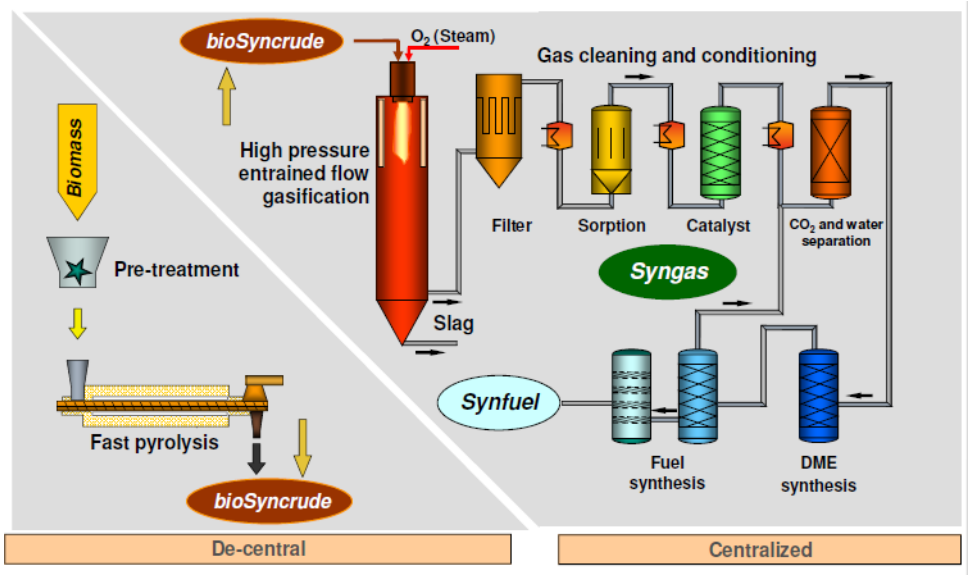

Figure 2.1: Bioliq®- process scheme [10]

The process can be divided into two main steps: regional and centralized. The regional (de-central) step aims to prepare the biomass by minimizing its volume and to produce energy dense biosyncrude® for storage and transport. The centralized step consists of gasification of biosyncrude® into tar-free syngas, followed by the subsequent processes like syngas treatment and cleaning, and the catalyzed synthesis of desired products such as fuel, as illustrated in figure 2.1. The concept was formerly called as BTL2, which means “biomass to liquid in two steps”. The concept was developed to lower the transportation cost per ton by producing biosyncrude® with energy density higher than that of straw bale. The difference between transport cost of straw and biosyncrude® is given in Table 2.1 [11].

Raffelt et al. (2006) suggests that, even though the distance between the pyrolysis plant and the central gasifier may be more than 170 km, the energy consumed by the transport of biosyncrude® can be negligible, for example if transportation is done by train [11].

Table 2.1: bioliq®- process scheme [10]

	LHV (GJ/t)	Density (Kg/m^3)	Energy Density (GJ/m^3)	Costs for transport 250 km by train
Straw	14.4	50 to 200	0.7 to 2.6	100 euro/ton
Pyrolysis liquids	7 to 22	1100	8 to 24	
Char	31	200 to 700	6 to 22	
Slurry with 30 % solids	14 to 25	1300	17 to 33	14 euro/ton

2.1 Biomass preparation and flash pyrolysis:

The pre-treatment of biomass is performed by so-called fast pyrolysis. Any kind of dry lignocellulosic biomass can be utilized in bioliq® process. KIT focuses on low-quality lignocellulosic biomass because lignocellulosic biomass is largely available in Central Europe, and it also minimizes the risk of food competition.

The biomass preparation for the fast pyrolysis is based on conventional drying and diminution processes which have been tested for various bio-materials at KIT. It was found that drying below 15% water content by weight is particularly desirable for storage without biological degradation [13]. It is also advantageous for increasing the brittleness and reducing the energy consumption for diminution. The dry bio-materials are reduced into particles smaller than 3 mm in size by a sequence of cutting and hammer mills. This finely ground biomass feed is essential for very high heat transfer rates in fast pyrolysis as suggested by Bridgewater and Peacocke [12].

The reduced biomass is transported into the flash pyrolysis reactor and is rapidly heated up to 500 ^{0}C with an excess heat carrier like sand, in the absence of air. In the bioliq® pilot plant, a pneumatic lift pipe, operates with hot flue gases produced by fast pyrolysis is used, in order to re-heat and lift the sand to the reactor. The simplified fast pyrolysis reaction of dry straw is represented by the following empirical equation [13a]:

$$C_6H_9O_4 \longrightarrow C_2H + C_3H_5O_2 + H_2O + CHO \quad (2.1)$$

Lignocellulose — Char — Pyrolysis Water — Non- condensable gases

Condensate

According to Bridgewater and Peacocke, (2000), any type of flash pyrolysis reactor can be used to prepare a bioslurry by pressurized entrained flow gasification [13a]. At KIT, a flash pyrolysis system with a twin screw mixer (TSM) reactor from Lurgi-Ruhrgas is being developed. The flash pyrolysis process with the TSM reactor is summarized in figure 2.2 [13b].

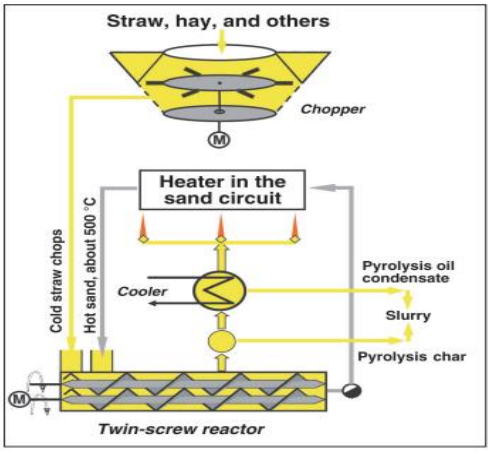

Figure 2. 2: Flash pyrolysis with TSM reactor for the production of pyrolysis oil and char scheme [13b]

The pyrolysis gas is withdrawn from reactor and the char is separated by a hot gas cyclone. Afterwards a large portion of vapours condenses to dark brown pyrolysis oil (the so-called bio-oil) that has a strong smell of smoke aroma. It is similar to traditional pyrolysis processes that are used for making charcoal; fast pyrolysis is more advanced process that can be carefully controlled to give high yields of liquid [13b]. This large fraction of liquid condensate can only be reached within few seconds by flash pyrolysis reactions and fast cooling of the products.

High condensate yield of 45 to 75% by weight can be produced with low char and gas yields. The char yield is in the range between 10 to 35% by weight. These proportions in the product yield depend on the biomass used as shown in the figure 2.3. Bio-oil with pyrolysis char particles could be a problem in combustion applications as the char contains ash and the flame would be unstable due to non-homogenous fuel mixture. Nevertheless, pyrolysis condensates with much char and ash are still suited for biosyncrude® preparation and subsequent gasification, due to several reasons: Primarily, the pyrolysis char increases the energy content of the bio-oil considerably by 30 to 80%. Secondly, the bio-oil quality requirements for pressurized entrained flow gasification are less when compared to combustion. Whereas the burner is very sensible to inorganic compounds even at levels below 1%, for the entrained flow gasifier high ash content is even acceptable in the gasification chamber to generate a protective slag layer as shown in figure 2.3 [14].

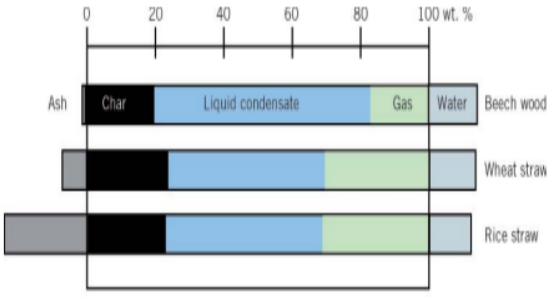

Figure 2.3: Product yield of fast pyrolysis using different feedstock in wt. % [13b and 15]

The non-condensable pyrolysis gases contain mainly CO and CO_2 in amounts between 30-55 % by volume; CH_4, H_2 and hydrocarbons in the amount of 10% by volume. The total energy content of pyrolysis gases is about 10% of the initial biomass energy, which can be used for reheating the circulated sand.

2.2 Biosyncrude® production and storage:

The main purpose of biosyncrude® concept is the preparation of a suitable feed for a large pressurized entrained flow Gasifier. There are good motives to produce the biosyncrude®:

- To achieve a single pyrolysis product with high energy density.
- Easy handling, compact storage and cheap transport
- A free-flowing bioslurry (see figure 2.4) that can be smoothly pumped into a highly pressurized gasifier with less effort [5].

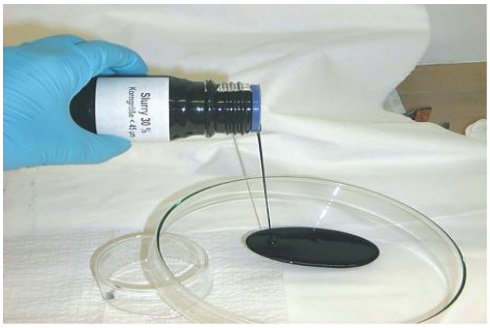

Figure 2.4: The biosyncrude, energy dense intermediate produced by pyrolysis products [13b]

Pyrolysis contains char 20-40% and bio-oil (condensate) 50-70%, and, together, contain up to 90% of the initial bio-energy. If only the bio-oil is used for gasification without char, about one-third of the bio-energy would not be accessible for syngas production. For this reason, the char is mixed with bio-oil by a colloidal mixer to generate a highly viscous, pumpable and energy dense suspension (so-called

biosyncrude® or bioslurry) [11]. The biosyncrude® with particle volume fraction up to 50% are free-flowing and pumpable, thus the char content may be as high as reasonably possible. Slurries with char particles in size of 10 µm or below allow higher loadings and remain homogenous for weeks or months, while in slurries with larger char particles sedimentation occurs within hours [10] [14].

A significant part of the pyrolysis char is the large aggregate of smaller porous char particles. De-agglomeration in a colloidal mixer can liberate a part of the condensates soaked up by the porous char particles, and let them surround the particles as a lubricant. It is essential to combine the following steps for successful biosyncrude® preparation: char reduction to less than 10 µm, de-agglomeration and homogenization of biosyncrude® in a colloidal mixer, mixing in large vessels to obtain desired composition throughout the suspension and preheating with waste heat from the process to reduce the viscosity before gasification.

2.3 Pressurized entrained flow gasification of Biosyncrude®:

The preheated biosyncrude® is transferred by pumps into highly pressurized entrained flow gasifier and atomized with pure oxygen at >= 1200 ^{0}C to a tar-free, low methane synthesis gas. The bioliq® entrained flow gasifier as shown in figure 2.5 is designed for operating pressures up to 80 bar, so that an expensive compression of the synthesis gas and larger gasifier volume is avoided [14]. Moreover, the gasifier is equipped with a special cooling screen taking the high ash content of the biomass into account. The ash pounds down as molten slag on the cooling shield, the slag coat protect the material from abrasion. The continuously draining slag is discharged after rapid cooling by water-quench [15].

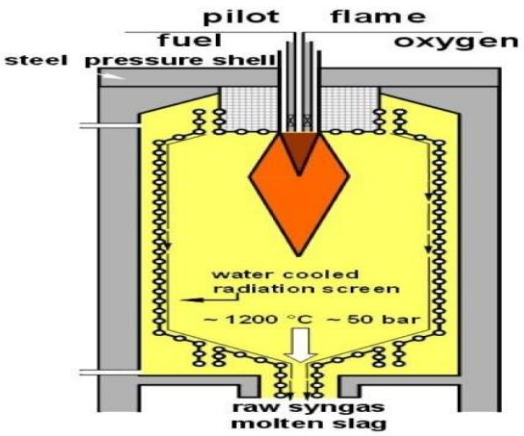

Figure 2.5: Scheme of a pressurized entrained flow gasifier with cooling screen [13b]

2.4 Gas purification and conditioning:

Syngas is a platform chemical that can be used in many applications like integrated gasification combined cycle (IGCC) power plants, or small combined heat and power (CHP) plants with stationary gas turbines. While moderate gas cleaning is necessary for these applications, a very efficient raw syngas cleaning and conditioning is required for a catalyzed synthesis.

The bio-syngas cleaning procedures for biogas have not yet been investigated so far on a larger scale but are included in the future program. In the pilot facility, a special hot gas cleaning system is applied. The working principle is the physical separation of particulates such as ash and char by means of particle filter, followed by the removal of HCl, H_2S, COS and alkaline by means of adsorption, and catalytic decomposition of NH_3, HCN and organic compounds at > 500 ^{0}C. The pre-purified synthesis gas is finally freed from CO_2 by a solvent wash and is then ready for the fuel synthesis step [13 a, b] [14] [15].

2.5 Fuel synthesis:

The conversion of synthesis gas into fuels on larger scale is state-of-the-art: via Frischer-Tropsh synthesis, dimethylether (DME) synthesis. For methanol synthesis, for instance a H_2/CO ratio of 2:1 would be achieved via a separate water gas shift reaction:

$$H_2O + CO \longrightarrow H_2 + CO_2 \qquad (2.2)$$

The preliminary work of DME synthesis at KIT has shown that adjustment ratio of 1:1 of H2/CO is not required. The DME is directly converted into fuels by catalytic dehydration, oligomerization and isomerization which are carried out at temperatures between 350 and 450^{0}C and a pressure of about 25 bar [13].

2.6 Comprehensive survey:

With approximately 7 kg air-dry straw, 1kg synthesis fuel can be produced in the bioliq®-process. Thereby ideally about 45% of the heat content of the biomass is converted into fuel. The waste heat of the process can be recycled to cover the full energy requirement. A division of the different energy flows is shown in the figure 2.6. In this case, the energy efficiency of the Fischer-Tropsch synthesis is given in percentage. [16].

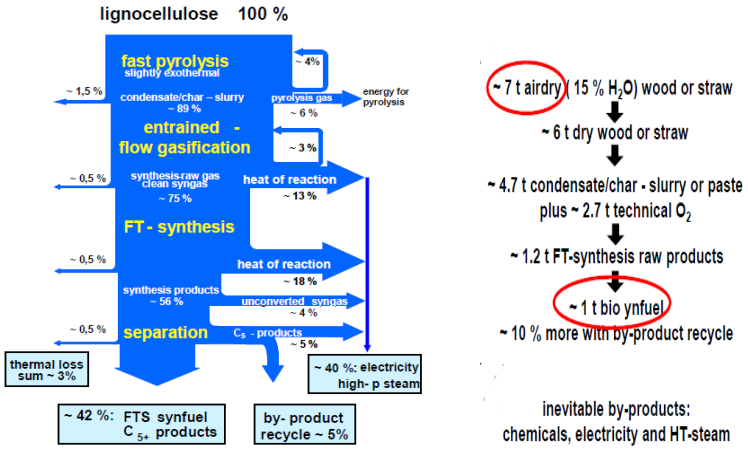

Figure 2.6: Summary of bioslurry gasification results [16]

Chapter 3: Literature Review

3.1 Pyrolysis:

Fast pyrolysis is a thermo-chemical process, where with high heating rates and temperature of about 500°C in absence of oxygen, biomass is converted into condensible pyrolysis vapours, gases and char particles [17].

3.1.1 Fast Pyrolysis of biomass:

Renewable energy is gaining importance regarding environmental and economic concerns over fossil fuels usage. Lignocellulosic materials are the most abundant renewable resources on earth [18]. Energy can be obtained from biomass either bio-chemically or thermo-chemically. In the bio-chemical process, pretreatment of biomass is imperative. The first step is the opening up the structure of the biomass cell wall and to allow the access of enzymes to cellulose and hemi-cellulose. Pyrolysis, gasification, and combustion are the three main thermo-chemical processes to get energy from biomass. According to Wornat, the burning of bio-oils produced by pyrolysis of biomass is more efficient than combustion and gasification. Bio-oil offers advantages in storage and transport and is a good source of chemicals [19] [20].

Pyrolysis is a chemical reaction in which thermal decomposition occurs in the absence of oxygen [21]. It is always the first step in gasification and combustion, in which partial or total oxidation of the substance occurs. It is mentioned in literature that the overall fast pyrolysis reaction should take place within 2s [22] [23]. The rate of thermal decomposition depends on biomass particle size and type, heating rate, final temperature, reactor configuration and presence of impurities. After volatilization, vapours and solid products are separated through cyclone before rapid quenching of vapours into liquid product called bio-oil. Gas is the main product (85%) in gasification, whereas bio-oil (70-80%) is the main product in fast pyrolysis. The yield of pyrolysis products such as syngas gas (mixture of CO and H2), bio-oil, and bio char (charcoal) would differ depending on the pyrolysis methods (conventional, fast, vacuum, flash, and ultra), biomass distinctiveness/characteristics (feedstock type, moisture content, particle size), and reaction parameters (rate of heating, temperature, and residence time).

There are four essential features to get bio-oil from fast pyrolysis:

- Very high heating rates (1000 °C/s)
- High heat transfer rates (600-1000 W/cm^2)
- Short vapor residence times (typically <2 s) which is already mentioned above,
- Rapid cooling of pyrolysis vapors and aerosols

Because the spirit of a fast pyrolysis process is the reactor, during the last two decades several different reactor designs have been explored to meet the rapid heat transfer requirements. Achieving very high heating and heat transfer rates during pyrolysis frequently require a finely ground biomass feed [24].

The production of bio-oil through pyrolysis is a thermodynamically non-equilibrium process. This process requires only a short residence time in a high temperature zone followed by rapid thermal quenching to produce a bio-oil that is also not at equilibrium [25The reactions result in the formation of larger molecules and accordingly increase the viscosity of the bio-oil [25] [26]. Because of the high oxygen (40-50 wt %) and water content (15-30 wt %) and the low H/C ratios, bio-oils cannot be used as transportation fuels directly without prior upgrading. Additional obstacles of bio-oil are the limited stability of the bio-oils under storage conditions due to the presence of unsaturated compounds and their low miscibility with conventional liquid fuels [27].

Several studies have been conducted on the rheological characterization of bio-oil with different feedstock. There are different parameters involved to investigate this characterization of bio-oil which is the aim of this study. Viscosity of bio-oils produced, is characterized by fluid temperature, residence time, water content, solids content, and quenching temperature.

3.1.2 State of fast pyrolysis technology:

The first oil price crisis paved the way for technical and scientific advancement in fast pyrolysis of biomass which was mainly performed by D.S. Scott and co-workers at the University of Waterloo, Canada [28]. The basic idea was to convert the renewable wood resources into liquid biofuels. Despite more than 30 years of development, there are no fast pyrolysis plants for a large-scale bio-oil production. The main obstacles in the production of commercial bio-oil fuels can be found in a number of reasons such as:

- High bio-oil costs combined with poor quality
- Even less amount of ash and char contents available in bio-oil are not suitable for higher combustion applications
- Chemical instability with sensitivity to phase separation
- Different feedstocks with different qualities
- Insufficient resources of lignocellulose feedstock in densely populated areas

3.2 Properties of Bio-oil:

Bio-oil is a liquid product of fast pyrolysis. Bio-oil can be recognized by different names like pyrolysis condensate, pyrolysis liquid; other synonyms found in literature are: wood tar, carbonization tar, tar oil. It is miscible with water, but not with hydrocarbons (heating oil). Bio-oil consists of volatile organics pyrolysis tar, moisture, pyrolysis water. Bio-oil can separate in two phases a heavier organic tar fraction with little water and a lighter aqueous phase with dissolved organics. Pyrolysis water consists of 50-80% water with 20-50% dissolved organic compounds [29].

Bio-oils, the main constituent of bioslurries, are a dark brown to black liquid with a wide range of viscosities (viscosity decreases with increasing water content). The smell is known from smoked ham. The depolymerization of the organic materials (cellulose, hemicelluloses and lignin) leads to a variety of different chemical compounds [30]. The liquid condensate consist of several hundred organic compounds like carboxylic acids, aldehydes, ketones, alcohols, phenols, esters, furans, pyrolytic lignin, sugar derivates, etc. and water. Only less than 60% of the individual components in complex bio-oil mixtures have been identified up to now [30] [31]. However, a general list of fast pyrolysis products identified by GC-MSD (gas chromatography-mass selective detector) has been reported to: (values in m- %) water 23.9; acids 4.3; alcohols 2.23; aldehydes and ketones 15.41; sugar derivatives 34.44; low molecular mass lignin 13.44; high molecular mass lignin 1.95; extractives 4.35. The fluctuation of these above mentioned values of all properties is +/- 10% range relatively [32].

Water is the most abundant single constituent with a yield range of 15-35 m-%, depending on the reaction water yield and the moisture of the feedstock [33]. Sugar and lignin derivates plus water contribute about 70 % to the bio-oil on weight basis. The density of the bio-oil is around 1200 kg/m^3. Because of the presence of the carboxylic acids, the pH-value is in the range of 3. The viscosity of bio-oil depends strongly not only on the water content, but also on FP process configuration, feedstock, age and storage conditions [35]. Zhang et al. pointed out that the viscosity values of bio-oil are in range of 70-350 mPa.s up to certain temperature range because it varies with temperature as well [31]. The HHV of bio-oil is in the range of 16-24 MJ/kg which corresponds up to 2/3 of the HHV of heating oil.

3.3 Significance of bio-oil viscosity:

Viscosity of a bio-oil is the measure of its internal friction/resistance of fluids which resists its flow. This is an important fuel property that should be considered in designing, processing, handling and transportation. Viscosity of bio-oil during operation of fuel injection equipment, particularly affects the fluidity of fuel at low temperatures. However, the quality and practical application of bio-oil as fuel is intimately dependent on its viscosity and the elemental compositions so lower viscosity is desirable [35]. In general, bio-oil has a high viscosity as compared to crude oil and diesel fuel [36] [37]. Pootakham and Kumar reported that the loading equipment of the petroleum product such as gasoline and diesel fuels has volume flow rate between 0.9 and 1.3 m^3/min, whereas bio-oil volume flow rate is 0.6 m^3/min and an operating pressure of 205 kPa for safety [38] [39] [40]. Bio-oil is more viscous than crude oil at room temperature; however its viscosity is very similar to that of crude oil in a temperature range of 35–45ºC [38] [39] [41] [42]. When the bio-oil is transported in a pipeline, the temperature of the pipeline should be maintained in the range of 35–45ºC to keep the viscosity similar to that of crude oil [38] [39].

Usually, high viscosity of fuel results in incomplete combustion and poor atomization. Injection nozzles and combustion chamber can clot by the formation of excessive carbon deposits. [43]. Hence bio-oils in their original form are not suitable for use in modern diesel engines. Because of the low thermal stability,

high acidity, high viscosity, low calorific value and poor lubrication characteristics that limit their use as transportation fuel [44] [45] [46]. Oasmaa stated that, the viscosity should be in the range of 10-20 mPa.s with a solids content of less than 0.1 wt% for engine application [47]. Bio-oils are entirely different from petroleum fuels so there is a necessity to establish fuel specifications for commercial application of bio-oils as liquid fuels. The specifications should contain the most significant properties such as viscosity, homogeneity, solid, lubricity, heating value, pH, stability, water, flash point, and ash [48].

The viscosity of bio-oil differs due to presence of water which has both negative and positive effects on the utilization and storage of bio-oils. During the combustion process, the negative effects are phase separation, lower heating value, increase of ignition delay, and reduction of combustion rates and adiabatic flame temperatures. Further, it leads to impulsive evaporation and consequent injection difficulties during the preheating process. The positive effects are viscosity reduction, lower pollutant emissions and better atomization. Moreover, OH radicals from water can inhibit the formation of soot and can also accelerate its oxidation [49].

Viscosity of the bio-oil is related to number of saturated bonds and fatty acid chain length. In general, the density of bio-oil being higher than that of water confirms that it contains heavy fractions [50]. Viscosity of bio-oil increases during storage, due to slow polymerization and condensation reactions. The presence of inhibitors (hydroquinone) can reduce the rate of increase in bio-oil viscosity. This reduction is caused by thermal polymerization reactions. Ageing increases the water content in bio-oil with time in accordance with the occurrence of condensation reactions [51]. The instability may be affected by the presence of alkali metals in the ash, which are being entrained by the char particles with the vapors. These alkali metals catalyze the polymerization reactions and thereby increase the viscosity [52].

3.4 Fluid Rheology:

It is important to model the fluid rheology correctly, particularly when non-Newtonian rheologies are concerned. The rheological properties of liquids handled in industrial processes can often change during the course of the process [53].

For Newtonians fluids, viscosity depends on temperature and pressure. At constant temperature and pressure, Newtonian behavior is characterized as follows [54]:

1. The shear stress is the only stress generated in simple shear flow.
2. The shear viscosity is independent of the shear rate.
3. The viscosity does not vary with the time of shearing and the stress in the liquid falls to zero immediately after the shearing is stopped.
4. The viscosities measured in different types of deformation (e.g., uni-axial extensional flow and simple shear flow) are always in simple proportion to one another.

Examples of Newtonians fluids are water, oil, glycerol, and sugar solutions. Dilute sludges such as unconcentrated activated and trickling-filter sludges also show Newtonian behavior.

In Non-Newtonian fluid, viscosity show deviation with shearing rate, such as paints, emulsions, most mineral slurries, latex, paper pulp, plastic melts, liquid foods, polymeric liquids, and concentrated wastewater sludge. One important thing to remember the viscosity of a non-Newtonian fluid is not a coefficient of the shear rate but a function of it and is called the apparent viscosity [55].

$$\mu_a = \frac{\tau}{\dot{\gamma}} \qquad \textbf{(3.1)}$$

Some exemplary curves are shown in figure 3.1:

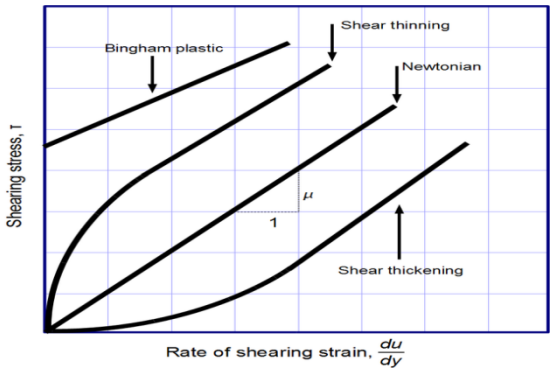

Figure 3. 1: Flow curves of Newtonian and non-Newtonian fluids [56]

3.5 Viscosity measuring instruments:

For rheometric measurements, common methods in fluid systems are:

- Capillary (or tube)
- Rotational

In this section, a brief summary of rotational viscometer especially rheometer is given. A viscometer is a device used primarily for the measurement of viscosity, while a rheometer is a device used for the measurement of rheological properties over a varied and extended range of conditions [57].

Rotational Methods:

In rotational methods, the fluid is constantly sheared between two surfaces, one or both are rotating. These devices have capacity to shear the sample for long period of time to monitor an equilibrium state or transient behaviour, under controlled rheometric conditions. In general, rotational methods are better suited for the measurement of gels, pastes and concentrated suspensions.

Rotational measurements are stress-controlled or rate-controlled. A constant torque is applied to the measuring tool in order to generate rotation in stress controlled measurements, and the resulting

rotational speed is then determined. The rotational speed can be converted into a corresponding shear rate with well-defined tool geometry. A constant rotation speed is maintained in rate controlled measurements and the resulting torque generated by the sample is determined using a suitable stress sensing device, such as a strain gauge or torsion spring. Some instruments have the ability to operate in either stress-controlled or rate-controlled modes [57].

Rotational Rheometer:

In rotational rheometer, fluid is sheared between rotating cylinders, cones, plates, or helix under controlled-stress or controlled-rate conditions. It is high-precision (as compare to simple rotational rheometer) continuously variable shear instrument in case of non-Newtonian fluids. The basic rotational system consists of four parts:

(I) a measurement tool with a well-defined geometry

(II) A device to apply a constant torque or rotational speed to the tool over a wide range of shear stress or shear rate values

(III) A device to determine the stress or shear rate response

(IV) Device to control temperature of sample fluid and tool

Most rheometers are available in one of three tool geometries: concentric cylinder, cone and plate, helix [57].

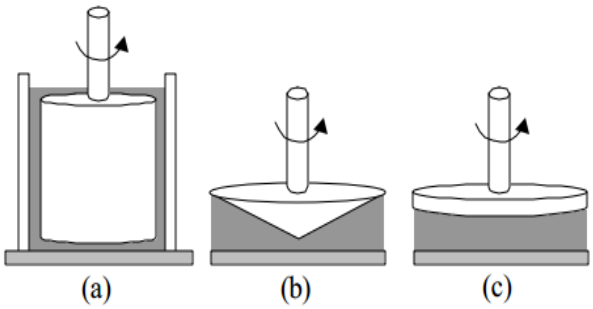

Figure 3.2: Schematic diagram of basic tool geometries for the rotational rheometer: (a) concentric cylinder, (b) cone and plate, (c) parallel plate [57]

3.6 Effect of water on bio-oil viscosity and other properties:

The amount of water in petroleum fuels is standardized because it forms a separate phase that can produce emulsion, cause corrosion and problems in burners. In fast pyrolysis bio-oil, water is either

dissolved or it exists as a micro emulsion. It cannot be removed by physical methods such as centrifugation [58]. Typically, the water content of the bio-oils is high (greater than 20% by weight), and it needs to be regulated because of its manipulation on other bio-oil properties as well as on the phase stability [59].

Fast pyrolysis bio-oils contain low-boiling (below 100 °C), water-soluble compounds, and for this reason, conventional drying methods or xylene distillation (ASTM D 95) cannot be used without a significant loss of organics [60] [61]. The water content of bio-oils can be analyzed by Karl Fischer titration [59].

Water affects physical properties of bio-oils. The density, viscosity, and heating value increase, when water content decreases. The increase in water content improves the stability of the bio-oil until it starts to separate out, typically at above 30% by weight. The high water content of the bio-oil lowers the adiabatic flame temperature and local combustion temperatures, which lowers the energy density, as well as, lowers the combustion reaction rates due to its relatively high vaporization temperature and high specific heat in the vapour phase [59].

It was already explained that the density, viscosity and surface tension varies a lot with the variation of water content. Here is little bit detail how these properties of fast pyrolysis bio-oil vary with percentage water.

The specific gravity is used in calculating weight/volume relationships, e.g. the heating value. The density is measured according to ASTM D 4052 at 15 °C using a digital density meter. The density of bio-oil is about 1.2 kg/dm^3 for water contents of approx. 25% by weight. Figure 3.3 shows the densities of various pine and forest residue bio-oils as a function of water content [59].

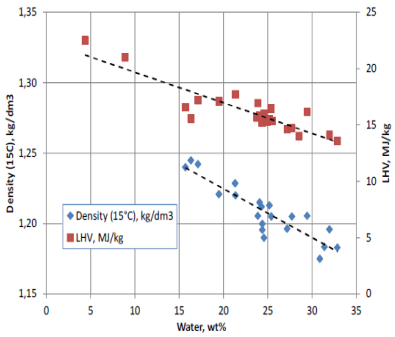

Figure 3.3: Density and heating value of pine and forest residue pyrolysis bio-oils as a function of water content [59]

The viscosity of standard fuel is typically measured as kinematic viscosity according to ASTM D445. The viscosity of bio-oils can also be determined as dynamic viscosity, using rotational viscometers [65]. Figure 3.4 shows the variation of viscosity with percentage of water.

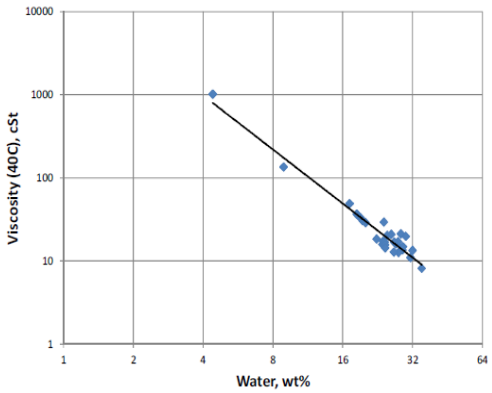

Figure 3.4: Viscosity pine and forest residue as a function of water content [59]

The surface tension of the liquid is a property that allows it to resist an external force. The relatively high surface tension of bio-oil presumably results from the high amount of water which has a high surface tension due to its strong hydrogen bonding [62]. For bio-oils, surface tension values of 28–40 mN/m at room temperature have been measured, whereas typical gas turbine fuels have surface tensions of 23–26 mN/m and diesel has a value of 28mN/m.

Table 3.1: shows the surface tension for some bio-oils measured using the pendant drop imaging technique [69].

Temperature (°C)	Drop run	Surface tension (mN/m) at 15 s	Equilibrium surface tension (mN/m)	Change (mN/m)
25	3	36.29	34.66	1.63
50	4	32.99	32.67	0.32
80	4	30.91	30.84	0.07

3.6.1 Physico-chemical properties of fast pyrolysis bio-oils:

Homogeneity:

Even though bio-oils are typically considered to be homogenous single-phase liquids, there are a number of reasons why two or more phases might be gone through during product recovery, handling or storage. If ignored, this phenomenon may cause serious problems in combustion applications. The water found in bio oils comes from two sources:

(1) The moisture that was present in the feedstock which causes the phase separation due to chemical composition

(2) The pyrolysis or chemically formed water which causes phase separation due to high water [63].

Phase-separation due to chemical composition:

The amount and type of neutral extractives (lipids, resin acids, etc.) in the wood feedstock causes the separation out of a distinct top layer from highly polar bio-oils [64, 65, 66, 67, 68]. Forest residues, in particular, yield a liquid with a 5–20 % by weight top phase that is low in polarity. The amount of top phase depends on the feedstock composition, as well as on the process and product collection conditions. Compared with the bottom phase, the top phase is low in water, oxygen, and density and high in heating value and solid content [59].

The operator of a pyrolysis plant will probably purchase wet feedstock from the biomass producer on a moisture-free basis, and then dry it to a moisture level that can be processed to produce acceptable bio-oil. However, the moisture in the feedstock is easily controlled by the extent of drying prior to pyrolysis. On the other hand, the capacity of the pyrolysis plant will increase as the moisture level of the feed decreases, due to the relatively large latent heat of vaporization of water compared to the heat required for pyrolysis. It is expected that the bio-oil will be sold on an energy basis (LHV). Because the LHV decreases with an increase in water content, it will not be advantageous to have high water content in the oil except to lower the viscosity to an acceptable value for good pumping and atomization prior to combustion. Too much water will cause the bio-oil to separate into two phases, a thin aqueous phase and a thick tar phase [57].

Phase separation due to high water content:

The difference in feedstocks play important role in the viscosity of the two oils. The water formed during pyrolysis is formed by dehydration reactions, which for the most part are linked to the char-forming reactions. The amount of char formed is partially a function of the alkali metal, content of the feed and of process variables that are primarily set by the pyrolysis configuration. [62]. Due to chemical activity in pyrolysis process, aldehydes can react with each other to form polyacetal oligomers and polymers. The polymer has limited solubility in water. In addition, the water content increases and the volatility of the oil decrease [69].

Bio-oils can be considered as microemulsions of water and water-soluble organic compounds with water-insoluble, mostly oligomeric, lignin-derived material. The ratio of these fractions depends on the feedstock, process conditions, and production and storage conditions. The water-insoluble fraction, mainly lignin-derived oligomers, usually accounts for about 20–25 wt% of the liquid (wet basis), while the water concentration typically ranges from 20 to 30 wt%.

Two-phase product with a larger aqueous phase and viscous oily phase may be produced if high-moist (greater than 10 wt %) feedstock is used. Alkaline metals, especially potassium, catalyze pyrolysis reaction, producing more water [65]. Hence, agro-biomass containing high amounts of potassium typically yields two phase product. Also, ageing reactions produce water, which might lead to the separation of an

aqueous phase when the total water content of bio-oil exceeds 30 wt%. The phase separation of bio-oil can also be induced by adding water intentionally which was observed in experimental work.

3.6.2 Others properties variation with percentage of water:

Bio-oil is chemically and thermally less stable than conventional petroleum fuels because of its high content of reactive oxygen-containing and unsaturated compounds. The chemical instability of bio-oil can be observed as increased viscosity over time, i.e., “ageing”, particularly when heated. The principal changes during ageing include a reduction in carbonyl compounds, aldehydes and ketones, and an increase in the heavy water-insoluble (WIS) fraction. There is usually no change in the content of volatile acids [59].

When pyrolysis bio-oil is heated, four stages are observed:

1. Thickening. The viscosity of the liquid increases mainly as a result of polymerization reactions

2. Phase separation. Water is formed as a by-product in ageing reactions. An aqueous phase separates out the heavy lignin-rich phase.

3. Viscous gummy-like “tar” formation from the heavy lignin-rich-phase if the temperature is raised above 100 °C for a long time.

4. Char/coke formation from the “tar” phase at higher temperatures, i.e., over 100 °C for a long time.

The stability of pyrolysis condensates towards phase separation into a heavy tar phase and a lighter aqueous phase decreases with increasing water content. Above 30 to 35 wt% water, phase separation occurs almost immediately after condensation; we could never obtain a stable bio-oil from air-dry cereal straw. Even for some initially homogeneous bio-oil phases from wood with around 25 % water, phase separation has been observed after several weeks or months [70]. Due to the instability of bio-oils, special care has to be taken in handling, transporting, storing and using the liquids. It can clearly be seen that the water content of the pyrolysis bio-oil has a major influence on the stability [67] [71].

The Higher Heating Value (HHV) and Lower Heating Value (LHV) of bio-oil are theoretically linear functions of the moisture content. Because the moisture content affects the heating value of the wet oil, it also affects the adiabatic flame temperature. The flame temperature is important because the available heat from the combustion is proportional to the difference between the flame temperature and the temperature of the exiting flue gases. The exiting flue gas temperature is a function of the heat recovery equipment [62].

The change in water-insoluble content correlates with increased molecular weight distribution and viscosity. The change in carbonyl content of bio-oil correlates with the change in viscosity measured by stability testing conducted at 80 °C over 24 h [72] [73].

3.7 Effect of solid content on bio-oil viscosity:

Solids [char] are important due to requirements of the combustion system in different applications with respect to clogging of nozzles, valves and filters. Solids can block small capillaries in injection needles or cause erosion in pumps or other equipment. Solid contents are influenced by the particle size and particle size distribution of the feedstock. High molecular weight polymerization products can be formed around solids and cause sludge formation in storage tanks. The amount of allowed solids depends on application. Large heavy fuel oil [HFO] boilers can tolerate solids up to 1% by weight and they even improve the combustion by raising the heating value and by stabilizing the combustion. Small light fuel oil [LFO] boilers cannot tolerate solid content above 0.1 wt%. Solid content below 0.5% by weight can be obtained, and obtaining solid content even below 0.1% by weight is technically feasible [72] [75].

Suspensions are generally solid-liquid mixtures, in which solid particles are dispersed in liquid phase. In the suspension rheology, viscosity of suspension (η_s) based on the viscosity of liquid (η_L) present in suspension. This ratio is called the relative viscosity (η_r):

$$\eta_r = \frac{\eta s}{\eta L} \qquad \textbf{(3.2)}$$

General influence on the relative viscosity is by the concentration of the solid, solid particle shape, and particle size distribution. In addition there are interactions between individual particles and solid [76].

Table 3.2: Approximate equations theoretically and empirically found to the concentration dependence of the viscosity in the suspension rheology for particles with spherical shape [76]

Author	Publication Year	η_r	Coefficient	Validity
Einstein	1906	$1+2.5C_v$	C_v: Volume concentration	C_v <1%
Batchelor	1970	$1+2.5C_v+6.5C_v^2$	C_v: Volume concentration	C_v <10%
Krieger-Dogherty	1959	$\frac{1}{\left(1-\frac{C_v}{C_{max}}\right)^{2.5*C_{max}}}$	C_v: Volume concentration C_{max}= Max. packing density	10 % < C_v< C_{max}
Quemada	1976	$\frac{1}{\left(1-\frac{C_v}{C_{max}}\right)^2}$	C_v: Volume concentration C_{max}= Max. packing density	10 % < C_v< C_{max}

During the 20th century, many approximate equations have been published, which describe the relationship between the relative viscosity (η_r) and the solid volume concentration (c_v). Some are based

on theoretical considerations, others are empirical approximations. The accuracy of such an equation often strongly depends on the type of solid, particle shape and solid concentration range from [81]. A brief overview of the table 3.1 is shown in figure 3.5.

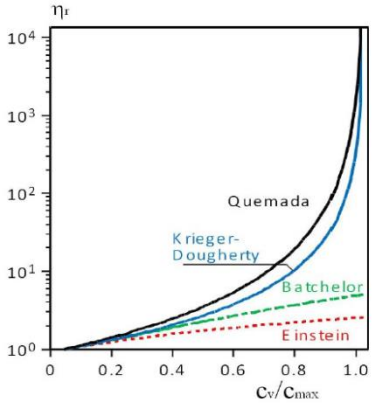

Figure 3.5: Concentration dependence of the relative viscosity for the given Table 3.1 [75]

Krieger-Dougherty:

$$\eta r = \left(1 - \frac{C_v}{C_{max}}\right)^{-B*C_{max}} \quad \textbf{(3.3)}$$

A model for describing the effect of particle on viscosity, where C_v is the particle volume fraction and C_{max} is a parameter representing the maximum packing fraction, and B is the Einstein coefficient. For ideal spherical particles B=2.5. Non-spherical or highly charged particles will exhibit values for B exceeding 2.5. The value of B is also affected by the particle size distribution. The parameter C_{max} is a function of particle shape, particle size distribution and shear rate. Both B and C_{max} may be treated as adjustable model parameters. The aggregate volume fraction (representing the effective volume occupied by particle aggregates, including entrapped fluid) can be determined using this equation if C_{max} is fixed at a reasonable value (e.g., 0.64 for random close packing or 0.74 for hexagonal close packing) and B is set to 2.5. In this case, C_{max} is the adjustable parameter and is equivalent to the aggregate volume fraction [57].

3.8 Effect of temperature on bio-oil viscosity:

The variation of viscosity with temperature follows an Arrhenius-type relationship. From literature, the variation of viscosity with temperature was studied in the range 20 ^{0}C to 80 ^{0}C. The natural log of dynamic viscosity versus reciprocal of temperature shows that the Arrhenius-type relation holds for wood samples [77].

The effect of temperature is normally fitted with the Arrhenius-type relationship that is shown below

$$\eta = a * e^{\frac{-E_a}{R*T}} \quad \textbf{(3.4)}$$

η= Dynamic viscosity in Pa.s

a= Pre-exponential factor (Pa.s)

T= Temperature in Kelvin

E_a= Exponential constant that is known as activation energy (J/mol)

R= Gas constant (J/mol/K)

The value of 'a' can be approximated as the infinite-temperature viscosity (η_∞) which is exact in the limit of infinite temperature. Hence, equation (3.11) can be rewritten in the following form:

$$\eta = \eta_\infty * e^{\frac{-E_a}{R*T}} \quad \textbf{(3.5)}$$

Equations (3.4) and (3.5) are basically equivalent. Although equation (3.4) normally appears in the literature, equation (3.5) gives a more accurate representation of the fluid since the pre-exponential value is better defined there. However, equation (3.5) is not yet in its simplest form [78].

Derivation of the Viscosity–Temperature Model:

It is widely accepted that natural logarithmic viscosity is directly proportional to the reciprocal value of the temperature. To increase the flexibility of this equation, constants **a** and **b** are introduced into equation (3.6) as shown below and can be linearized by taking the natural logarithm on both sides of the equation:

$$ln(\eta) = ln(a) + \frac{b}{T} \quad \textbf{(3.6)}$$

ln (a) is the intercept at the ln(η)-axis and b is the slope of the linear graph [78]. Viscosity data for the four points from 20°C to 80°C at 50 rpm for fluid sample was fitted with equation (3.6) using Microsoft Office Excel, and the R-squared value was estimated.

3.9 Heat exchange:

Heat exchange is an important process in chemical engineering. The most common device for heat exchange is, as one might expect, a "heat exchanger" [79]. It is defined as "A heat exchanger is a device that is used to transfer thermal energy (enthalpy) between two or more fluids, between a solid surface and a fluid, or between solid particulates and a fluid, at different temperatures". In heat exchangers, there are usually no external heat and work interactions. Typical applications involve heating or cooling of a fluid stream and evaporation or condensation of single or multi-component fluid streams. In other applications, the objective may be to recover or reject heat, or sterilize, pasteurize, fractionate, distill, concentrate, crystallize, or control a process fluid [80].

There are different types of heat exchangers. Heat exchangers can be classified according to:

- Heat process
- Number of fluids
- Surface compactness
- Construction
- Flow arrangements

Common examples of heat exchangers are shell-and tube exchangers, automobile radiators, condensers, evaporators, air pre-heaters, and cooling towers. If no phase change occurs in any of the fluids in the heat exchanger, it is sometimes referred to as a sensible heat exchanger. There could be internal thermal energy sources in the heat exchangers, such as in electric heaters and nuclear fuel elements. Combustion and chemical reaction may take place within the heat exchanger, such as in boilers, fired heaters, and fluidized-bed exchangers. Mechanical devices may be used in some heat exchangers such as in agitated vessels, and stirred tank reactors. However, in a heat pipe heat exchanger, the heat pipe not only acts as a separating wall, but also facilitates the transfer of heat by conduction and convection. In general, if the fluids are immiscible, the separating wall may be eliminated, and the interface between the fluids replaces a heat transfer surface, as in a direct-contact heat exchanger [80].

In all types of heat exchangers, the rate of heat transfer is controlled by the two variables, driving force (temperature difference) and resistance. Since the process sets the temperature of the fluid, a heat exchanger is designed to economically reduce the resistance [79].

3.10 Important numbers in H.E calculations:

3.10.1 Reynolds number:

A dimensionless group that expresses the ratio of the inertial forces to the viscous forces is known as Reynold number.

$$\boldsymbol{Re = Vd/\nu} \qquad \textbf{(3.7)}$$

Where d is a characteristic dimension (e.g., particle size or pipe diameter), v is a typical fluid speed, and $\boldsymbol{\nu}$ is the kinematic viscosity of the fluid. The transition from laminar to turbulent flow is characterized by high Re values [57].

Re< 2300 Laminar flow

Re> 2300 Turbulent flow

3.10.2 Prandtl number:

The Prandtl number is a dimensionless number, defined as the ratio of momentum diffusivity (kinematic viscosity) to thermal diffusivity [81]. That is, the Prandtl number is given as:

$$\mathbf{Pr} = \frac{\textbf{Viscous diffusion rate}}{\textbf{Thermal diffusion rate}} = \frac{\nu}{a} = \frac{cp * \mu}{k} \quad \textbf{(3.8)}$$

Where μ= Dynamic viscosity, ν= Kinematic viscosity, a= Thermal diffusivity, ρ= Density, k= Thermal conductivity, C_p= Specific heat

Pr<<1 means thermal diffusivity dominates

Pr>>1 means momentum diffusivity dominates

3.10.3 Nusselt number:

The Nusselt number (Nu) is the ratio of convective to conductive heat transfer across (normal to) the boundary of the fluid. Convection includes both advection and diffusion. Named after Wilhelm Nusselt, it is a dimensionless number. Nusselt number close to one, if convection and conduction magnitudes are similar, is characteristic of turbulent or laminar flow. A larger Nusselt number corresponds to more active convection, with turbulent flow typically greater than 2300.

$$\mathbf{Nu_L} = \frac{\textbf{Convective heat transfer}}{\textbf{Conductive heat transfer}} = \frac{\mathbf{UL}}{\mathbf{k}} \quad \textbf{(3.9)}$$

Where L is the characteristic length, k is the thermal conductivity of the fluid; U is the convective heat transfer coefficient of the fluid [81].

For Internal Flow:

Laminar pipe flow:

For Re<2300 [81]

$$\overline{Nu} = \left\{ 3.66^3 + \left[1.62^3 + 0.293 \left(Re \frac{d}{L} \right)^{\frac{1}{2}} \right] Re.Pr.\frac{d}{L} \right\}^{\frac{1}{3}} \quad \textbf{(3.10)}$$

Turbulent pipe flow:

For Re>2300>10^6 [81]

0.5<Pr<10^4

0<<d/L<1

$$\overline{Nu} = \left[\frac{\xi}{8}.\frac{(Re-1000)Pr}{1+12.7\sqrt{\frac{\xi}{8}}\left(Pr^{\frac{2}{3}}-1\right)}\right]\left[1+\left(\frac{d}{L}\right)^{\frac{2}{3}}\right] \quad \textbf{(3.11)}$$

$$\xi = (1.82.\log Re - 1.64)^{-2}$$

3.11 Plant shut down reason in KIT bioliq® plant:

The heat exchangers were shut down because the temperature after the heat exchangers rose constantly until it was above design value. This tendency was still observed when increasing the cooling water flow rate. When ethylene glycol was added to the tar cycle, the intended temperature level could be kept in normal range again. That's why it was concluded that the heat exchangers work well for ethylene glycol but not so much for tar.

3.12 Geometrical and process data availability:

The geometric and process data which was available for the investigation of W32402 (parallel flow H.E) and W32403 (counter flow H.E) is summarized as:

- The temperature at the inlet and outlet of the heat exchanger were given.
- The inlet and outlet temperatures of parallel flow H.E are correct but there is a problem at the outlet of counter flow H.E. It may be due to the disorderness of thermocouples or due to other systematic error.
- Mass flow rate of hot (ethylene glycol and organic tar) and cold fluids (water) were also provided by bioliq® pilot plant.
- The geometric parameters are provided by the manufacturing company Lurgi. Mainly the geometric parameters include length, thickness, outer diameter and number of tubes is mentioned. These are the major parameters that were used to calculate area, Reynold number, Prandtl number and Nusselt number. The design values of mass flow rate and specific heat were also given by the Lurgi.

3.13 Flow diagram:

There were two heat exchangers that were connected in series as shown in the figure 3.6. Heat exchanger W32402 was parallel flow heat exchanger and W32403 was counter flow heat exchanger. Red line indicates the hot fluid (organic tar or ethylene glycol) that is inside of the tube and blue line indicates the cold fluid which was water.

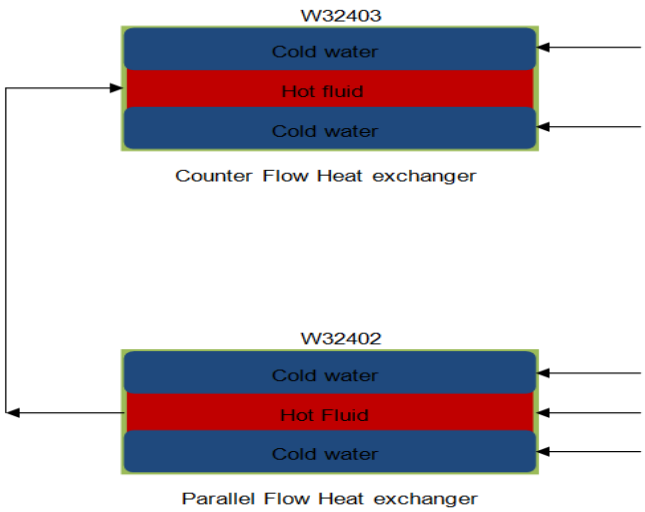

Figure 3.6: Flow diagram of heat exchangers of bioliq® plant KIT Karlsruhe, Germany

Chapter 4: Methodology

This chapter describes the experimental setup, material and material properties, experimental strategy and the method used in this study. The basic parameter measured is viscosity. The variables are fluid (organic condensate) temperature, water content and solid content.

4.1 Experimental setup:

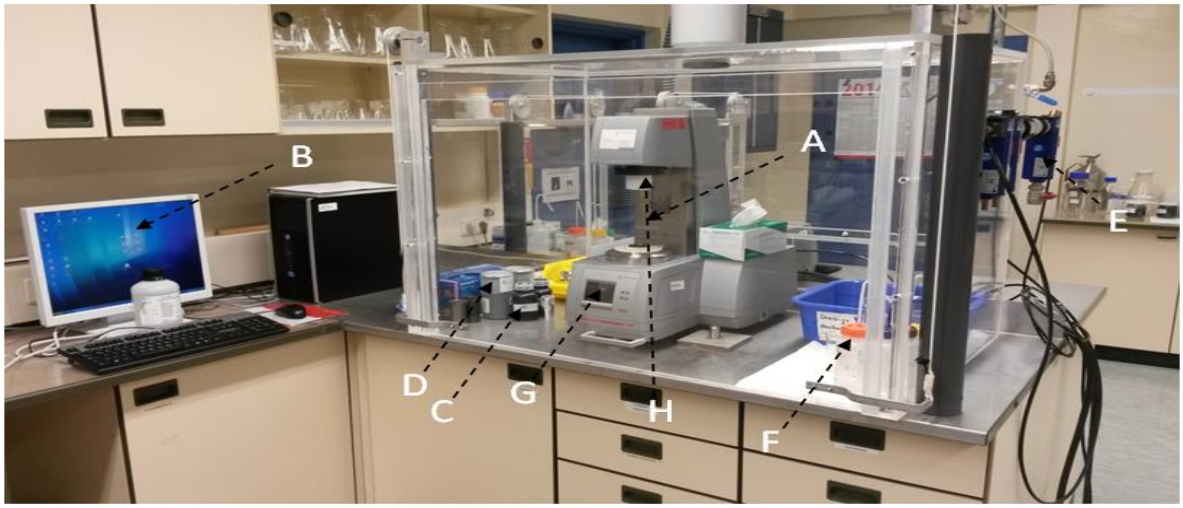

Figure 4.1: Experimental setup: A=mounting, B= computer with rheoplus software, C= sample from bioliq plant, D=spindle covering, E=pneumatic system for air pressure, F= methanol for cleaning, G= display of rheometer, H= covering to protect rheometer casing where spindle is attached

The experimental setup used in this study is shown in figure 4.1. All experiments are carried with this rheometer and samples have to take in the measuring beaker (up to the yellow mark on the top of the beaker). Place the beaker in the holder of the rheometer as shown in the figure 4.2 and screw it tightly .In case of a missing mark, it should be drawn with a paint stick 70 mm from the surface of the beaker. This instrument is connected to a computer by electrical wire signals which transform the mechanical action into electrical signals and show us in a graphical form using software called “rheoplus”. We fix the spindle with above coupling attached just below the side of mounting, which can slide up and down. Check that the mark on the coupling is in line with the spindle when the measuring system (helix spindle for slurries, cylindrical spindle for solid free fluids) is attached with coupling as shown in figure 4.2. Pneumatic system is also attached with rheometer in order to have a proper check on the pressure of air supply (i.e. 5 bars in our case). There is a weight measuring instrument for measuring the weight of solid particles and water in the experiments.

Figure 4.2: Rheometer accessories used in experiments

4.2 Material and material properties:

- Wheat straw biomass:

Sufficiently dry lignocellulosic biomass like wood or straw below 15 wt.% moisture can be stored without biological degradation. The dry biomaterials are diminuted in two steps into small particles of < 3 mm in size. The energy required for diminution is reduced at lower moisture. Biomass particles with a characteristic length of < 0.5 mm (sphere diameter, < 3 mm; cylinders, < 2 mm; plates, < 1 mm) which are equivalent to a specific surface of > 2,000-m^2/m^3 are used. Organic condensate of wheat straw sample 2014-1313 obtained through KIT bioliq® plant is analyzed in this study.

- Modular Compact Rheometer MCR 102, Fa. Anton Paar
- Helix-spindle, ST24-2HR-37/120 SN29240, Fa. Anton Paar as shown in figure 4.3.
- Cylinder-spindle, CC27-SN27965, Fa. Anton Paar

Figure 4.3: a) Cylindrical spindle CC27-SN27965, Fa. Anton Paar, b) Double helix spindle ST24-2HR-37/120 SN29240, Fa. Anton Paar

- **Straw Char:** The solid particles used for analyzing the effect of solid on viscosity are unmilled straw char with particle sizes given in Table 4.1. Unmilled char so called bioliq char obtained from the fast pyrolysis step of bioliq process. Small part of the heat carrier of fast pyrolysis (sand) is

carried away with the product (char). Therefore, the particle size measurement of unmilled char gives extreme particle sizes up to 525 micrometer because of the coarse sand particles.

Table 4.1: Particle diameters of un-milled straw char

Char	X_5	X_{50}	X_{95}
Unmilled straw	**10 µm**	**20 µm**	**70 µm**

- Viscosity Standard, from Brookfield (5000 Fluid, Viscosity 4980 mPa * s, T = 25 ° C, Lot Number: 080604)
- **Water:** It is used for analyzing the effect of water on viscosity when it is changed from certain percentage like 12.6%, which is already present in the sample, to 17% by weight. For water addition in fluid sample 2014-1313 pipette tube was used to control the percentage of water.

4.3 Experimental strategy:

This study aims to get a model for viscosity as a function of different parameters like fluid temperature, water content and solid content in our case. In order to accomplish this goal, viscosity is measured by rheometer and the parameters are varied as:

- Solid loading: solid concentration of 10, 10.5, 11, 11.5, 12, 12.5, 13, 13.5 and 14 percent by weight
- Water content addition: water is added in 12.6, 13, 13.5, 14, 14.5, 15, 15.5, 16, 16.5, 17 percent by weight
- Fluid temperature: temperature range discussed in this study is 20^0C, 40^0C, 60^0C and 80^0C
- Beaker filling level: 70mm which is mentioned by yellow line in beaker
- Helical spindle with correction factor of 88 is used and variation of speed is from 1 to 500 rpm.

The different range of water content was selected from the studies of literature used for wood and forest residue, the maximum value of water is up to 30%. As water improves the stability but it also forms two phases after this limit. For wheat straw this value is up to 20 to 25% as investigated in bioliq® plant but from experiments as illustrated in chapter 5, the range is 12.6 to 17 wt. %. Temperature range is selected from previous studies and the range from 20^0C to 80^0C is suitable for investigation. As far as, solid content is concerned; Krieger-Dougherty was selected since it is valid for solid contents higher than 10 percent. Higher values of solid contents could be selected as well but at higher values of solid content, the deviation increases. For that reason, the lower range of solid content is selected.

4.4 Procedure technique:

Dynamic viscosities of sampled fluid are determined by the rheometer MCR 102 from Anton Paar which has helical spindle system as we have mentioned in the material section earlier. For all measurements,

we used helical spindle due to its high accuracy of viscosity values and to avoid turbulent rheological regime. The accuracy deviation of helical spindle with cylindrical spindle was investigated already in KIT and it is in the marginal error of <= 7% [82].

All samples 2014-1313 from the same campaign and same material (wheat straw) were stored at room temperature in glass or plastic jars and mixed thoroughly by shaking the respective sample vessel/jar before filling the rheometer measuring cup. Then the spindle was inserted and is automatically detected by the software of the rheometer/viscometer. Organic condensate sample 2014-1313 has less sedimentation and weak turbulent flow behavior at high shear rates and elevated temperatures as compared to bio-slurries. Speed of helical spindle is chosen 50 rpm to avoid the turbulent flow regimes and temperature increase consequently increases the viscosity which is explained well in result section.

Viscosity determination:

The measurement of viscosity is very important for the characterization and determination of the flow behavior of the bio-oil. As described above, the analysis of the dynamic viscosity was conducted using the viscometer model MCR 102 by Anton Paar. The viscometer was equipped with a stirrer spindle (also called double helix spindle) as a measurement system. The spindle has a structure like a small spiral agitator with a length of about 150 mm. The dynamic viscosities obtained by measurements of helical spindle cannot be considered as absolute values but only relative ones. This was due to the fact that geometry of the helical spindle is not well-defined in comparison with cylindrical spindle. However, this is sufficient to get a comparison of viscosities of the bio-oil.

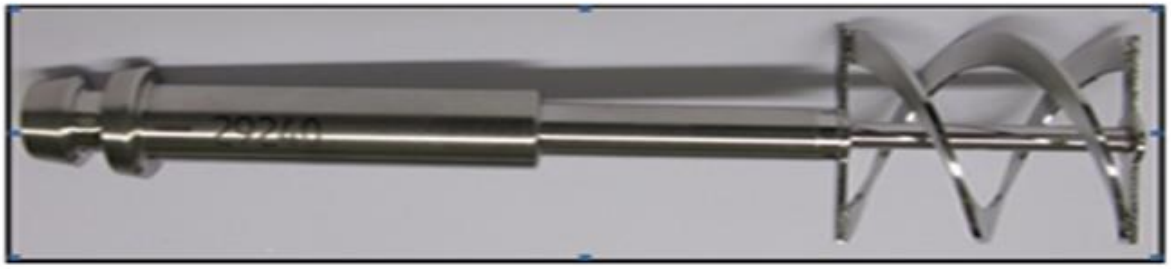

Figure 4.4: Double helix measuring system

All rheological profiles shown in the results section were generated in accordance with the current standard operating procedure test routine.

Device: MCR102 SN81023202, USB1: = MCR102 SN81023202

Measuring system: ST24-2HR-37/120 SN29240

Measuring position: 0 mm

Measuring cell: C-PTD200-SN81021734

The measurement method is divided into the following four sections as shown in Table 4.1:

Table 4. 2: Measurement sections of rheometer

Section	Measurement points	Measurement profile	
		Rotational speed n (1/min)	Temperature (0C)
Section 1	600	500	20
Section 2	180	0	20
Section 3	5	1	20
Section 4	40	1 to 500	20

Section 1: Here, the speed n = 500 rpm was kept high to achieve better mixing. After stabilization phase, for 2 minutes hold time at the desired test temperature +/- 0.1 ° C preheating of the sample is done. 10-minute pre-heating for homogeneous mixing of the sample takes place.

Section 2: For the elimination of initial shear strains it is necessary to give 3-minute rest period.

Section3: This section is for elimination of a start up shear strain when the rotation starts again

Section 4: There are 40 measured values (torque) depending on the speed (n = 1 ... 500 rpm) generated. These are the actual viscosity values.

Chapter 5: Results and discussion

Bioliq® Process analytics provides bio-characterization and rheological characterization, which is a key process parameter in this analysis. Due to the presence of solid content in our sample, determination of the viscosity of bio-oil is required. The effect of different parameters like water, solid and fluid temperature on viscosity is going to be characterized. During the measuring process, dispersion of the solid particles needs accurate determination of the viscosity of sampled fluid 2014-1313. The viscosity values are determined at low speeds deviated in a margin of error of ≤ 7% in helix spindle measuring system as compared to cylindrical measuring system. Therefore, spiral-shaped measurement system (" double helix screw") has been used [82].

The determination of viscosity through rheometer is possible with defined spindle geometries in the measuring system for example by the use of cylindrical, spiral or double helical spindle. There are usable spindle geometries that can be used to measure the viscosities however this study focuses on the helical spindle geometry. In these experiments, helical spindle has been used because it is more accurate than cylindrical spindle and the presence of suspended particles in the fluid is higher [82]. The values obtained through helical spindle are relative viscosity values therefore a correction factor of 88 is used.

It was observed that the use of a cylindrical spindle for viscosity determination is applicable only for homogeneous samples or with low solid contents. Absolute measuring systems are not suitable for determining the viscosities of bio-oil with higher percentage of solid content, as these tend to form two phase system within a very short time. Helical spindle enables the determination of viscosity of the fluids more accurately even with high percentage of solid contents. The threshold limit from this study was concluded to be 14% at 60 and 13%at 80^0C. After that, the sudden increase in viscosity and resistance to flow took place which is more effective with more solid contents as shown in figure 5.7, 5.9 and 5.11.

The determination of viscosity through rheometer is possible with defined spindle geometries in the measuring system for example by the use of cylindrical, spiral or double helical spindle. There are usable spindle geometries that can be used to measure the viscosities however this study focuses on the helical spindle geometry. In experiments, helical spindle has been used because it is more accurate than cylindrical spindle especially with higher amount of suspended particles [82].

It was observed that the use of a cylindrical spindle for viscosity determination should be the method of choice only for homogeneous samples with low solid content [82]. The use of a measuring system such as the helical spindle enables the determination of viscosity for fluids with a high solid content with more accuracy. Due to the exertion of a turbulent flow profile at higher speeds, the helical spindle should not be used at higher rotational speeds because increase of viscosity occurs at higher speeds as shown in figure 5.4a&b. Approximately at 400 rpm turbulent effect is prominent.

5.1 Model 1: viscosity at different temperatures:

Temperature plays a significant role in changing the viscosity of bio-oil. As temperature increases, the viscosity of sampled fluid (wheat straw organic condensate) reduces rapidly as shown in the figure 5.1. The applied temperature not only provides sufficient energy to break down the internal structure within the bio-oil very rapidly by reducing attraction forces between molecules; however, it also endorses molecular interchange.

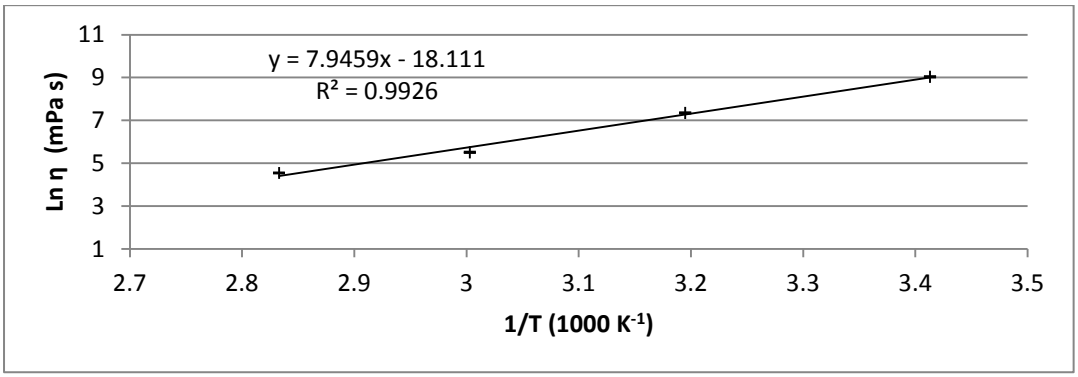

Figure 5.1:Temperature dependency of wheat straw bio-oil

Dynamic viscosity is plotted as **ln η** and temperature is taken as 1/T in Kelvin. It is clear from figure 5.1 that at higher temperatures the viscosity value is decreased. Viscosity is a function of temperature, solid content, water content etc, and it also related to aging issues of bio-oils. So at room temperatures for example at 20 ^{0}C the viscosity values are quite high because the heat which is provided in form of temperature is not enough to reduce its internal structure or to make it flow easily. As can be observed from the graph, when the temperature reaches from 20 to 80 ^{0}C the internal structure of molecules is going to allow the sampled fluid to reduce its dynamic viscosity as shown in figure 5.1. Viscosity and fluid temperature profile shows Arrhenius-type-relationship in figure 5.1 where the viscosity of the bio-oil is linearly decreased with increasing temperature. This pattern of temperature profile is similar as observed from previous studies of IKFT Karlsruhe [82].

Arrhenius equation is given as follows:

$$\boldsymbol{\eta} = \boldsymbol{a} * \boldsymbol{e}^{\frac{\boldsymbol{b}}{\boldsymbol{T}}} \quad \textbf{(5.1)}$$

It is widely accepted that natural logarithmic viscosity is directly proportional to the reciprocal value of the temperature. Equation 5.1 can be written in the form of 5.2 and can be linearized by taking the natural logarithm on both sides of the equation:

$$\boldsymbol{ln}\,(\boldsymbol{\eta}) = \boldsymbol{ln}\,(\boldsymbol{a}) + \frac{\boldsymbol{b}}{\boldsymbol{T}} \quad \textbf{(5.2)}$$

Ln (a) is the intercept at the ln (η)-axis and b is the slope of the linear graph [78].

The model equation obtained from this figure 5.1 is given below with a relative value of standard deviation of 3% for all data points. The equation and R^2 through curving fitting on Excel 2007 is given below:

$$\mathbf{y = 7945.9x - 18.111}$$
$$\mathbf{R^2 = 0.9926}$$

So the actual model is given in Arrhenius formation is

$$\boldsymbol{\eta = 3x10 - 3 * e^{\frac{7945.9}{T}}}$$

When the developed is compared with other models like standard model of viscosity and temperature whose R^2 is 1, it was observed as shown in figure 5.2 that wheat straw shows similar behavior of dynamic viscosity vs. temperature to beach wood.

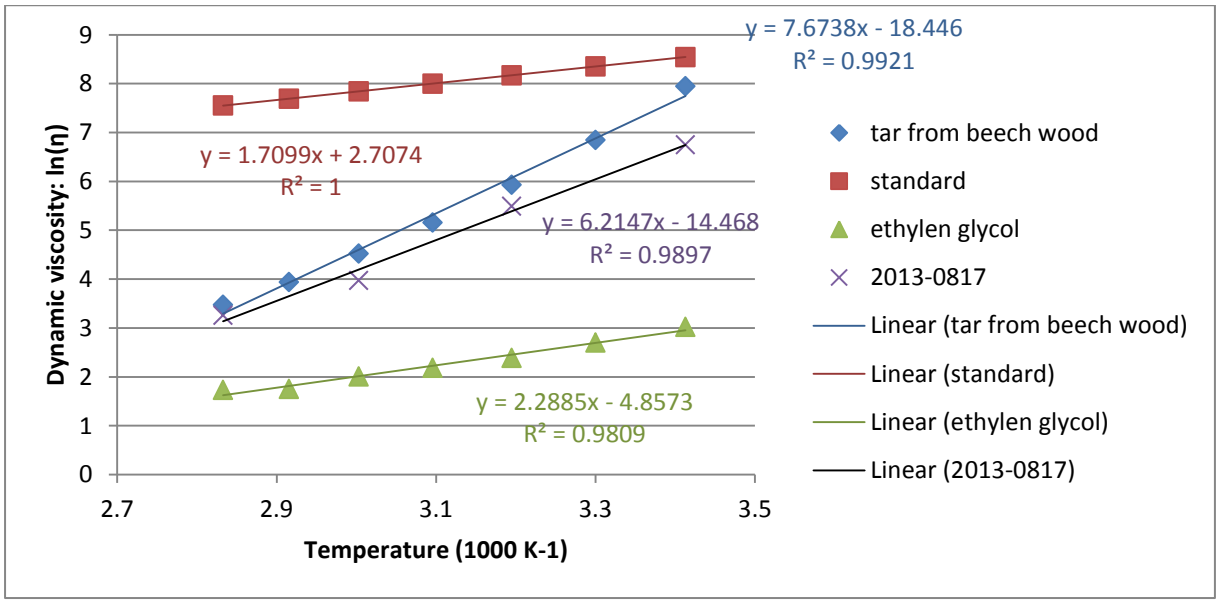

Figure 5.2: model of different sample of pyrolysis oil [83]

It is clear that homogeneous liquids of bio-oils exhibit an Arrhenius-like temperature curve, which means that the logarithm of viscosity increases proportional to 1/T. However, this is also true for highly-loaded suspensions. All plots are linear and almost parallel to each other by the comparison of figure 5.1 and 5.2.

R^2 is the first indication of the goodness of the curve fitting. But statistical analysis of regression like confidence interval of a model is both important and better indicators to describe the precision of a model and evaluate its validity. Mean values of viscosity with confidence interval of 95% have been plotted by using Predint function of MATLAB as shown in the figure 5.3.

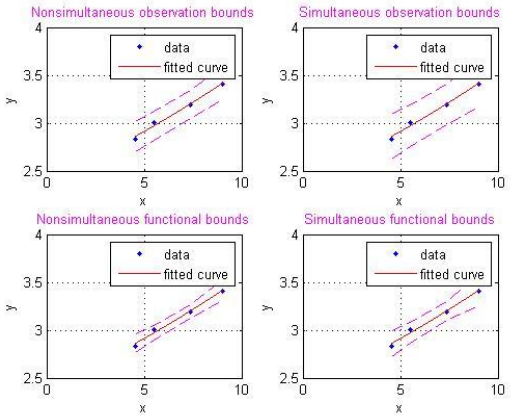

Figure 5.3: Arrhenius plot with confidence interval of 95%

The points are plotted in this format in MATLAB:

P11 = Predint (fitresult, x, 0.95,'observation','off');

P12 = Predint (fitresult, x, 0.95,'observation','on');

P21 = Predint (fitresult, x, 0.95,'functional','off');

P22 = Predint (fitresult, x, 0.95,'functional','on');

Observation means Bounds for a new observation (default) and functional Bounds used for the fitted curve. Off represents non-simultaneous bounds (default) and on represents simultaneous bounds as shown in figure 5.3.

Table 5.1: Upper and Lower bound variations at four points

Points (x values)	P1=2.832	P2=3.003	P3=3.195	P2=3.41
Upper bound(Y+)	3.0205	3.1203	3.3421	3.5894
Lower bound(Y-)	2.6975	2.8202	3.0507	3.2469

So the whole model is valid in between these values because these are detected by confidence interval of 95%.

Rotational speed of the spindle is important parameter in rheological characterization of bio-oils, because it has been observed in experiments that speed affects the dynamic viscosities of the sample fluid 2014-1313 as shown in the figure 5.4a&b. The deviation of accuracy of viscosity values determined by helical spindle at low speeds is in a margin of error of ≤ 7% [82]. High speeds lead, especially at higher

temperatures with helix spindle measurement systems, to a turbulent rheological regime as shown in figure 5.4b. The values for the relative viscosities of the tar samples are therefore determined at a speed of n = 50 rpm, so it was assumed that at this speed no turbulent flow behavior will occur and the flow is considered to be approximately Newtonian because there is no major deviation of viscosity values observed after 50 rpm.

To analyze the behaviour of speed on pyrolysis oil of wheat straw, a plot of viscosity vs. spindle speed is constructed automatically by rheoplus software. Viscosity is plotted along the y-axis and speed (RPM) along the x-axis. The slope and shape of the curve indicate the type and degree of flow behavior, steeper slope as it is from 0 to 50 rpm shows more deviation from Newtonian behaviour than from 50 to 500 rpm as shown in the figure 5.4a&b . The profile of viscosity with speed shows that bio-oil follows non-Newtonian behaviour. In non-Newtonian fluid categories, figures 5.4a&b follows pseudo-plastic fluid behaviour in which shear thinning takes place. At high speed and high temperature, turbulent flow regimes occur which cause the increase of viscosity as shown in the figure 5.4b. It is cleared that after 50 rpm there is small deviation of viscosity with speed but before 50 rpm, fluctuations are high.

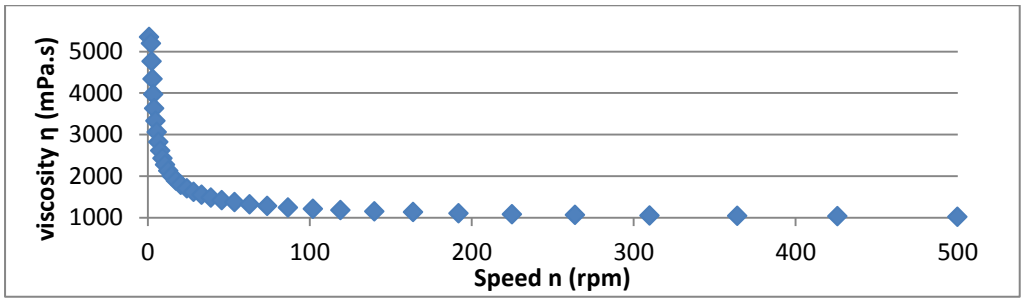

a)

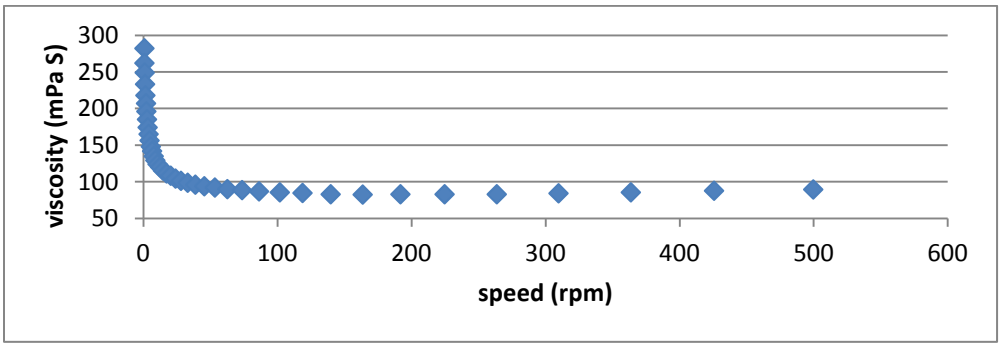

b)

Figure 5.4: Viscosity profile with speed a) without turbulent flow around 500rpm and 20 ^{0}C b) with the indication of turbulent flow around 500 rpm and 80 ^{0}C

The reduction of viscosity caused by temperature is far more apparent as compared to shear rate. As temperature increases, the viscosity of bio-oil reduces rapidly and then, the bio-oil's viscosity started to show temperature independence effect. The applied temperature not only provides sufficient energy to break down the internal structure within the oil very rapidly by reducing attraction forces between molecules, however, it also promotes molecular interchange. Eventually, the reduction of internal structure stabilizes by the increase of molecular interchange. In the overall view, this viscosity temperature profile is known as Arrhenius-type-relationship where the viscosity of the bio-oil is exponentially decreased with increasing temperature. This viscosity-temperature profile is presented in figure 5.5.

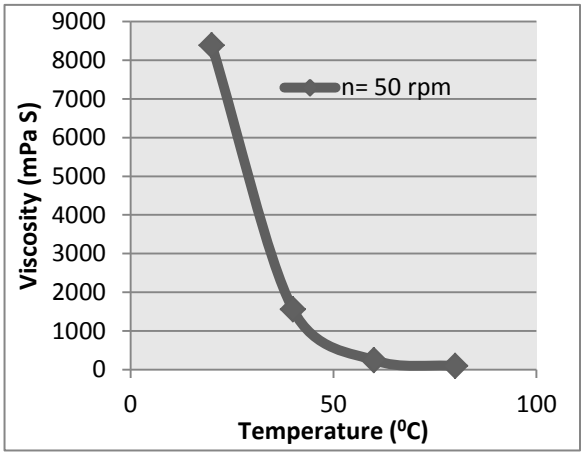

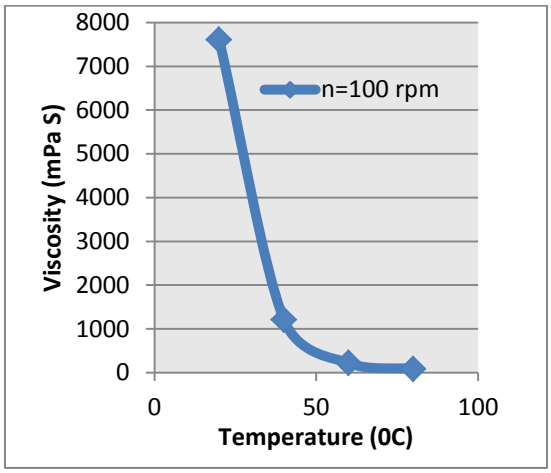

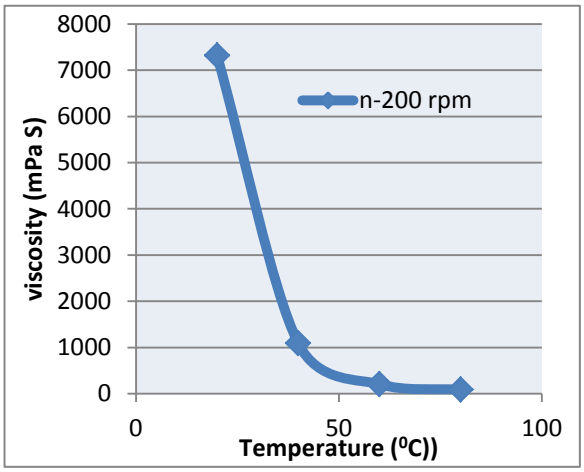

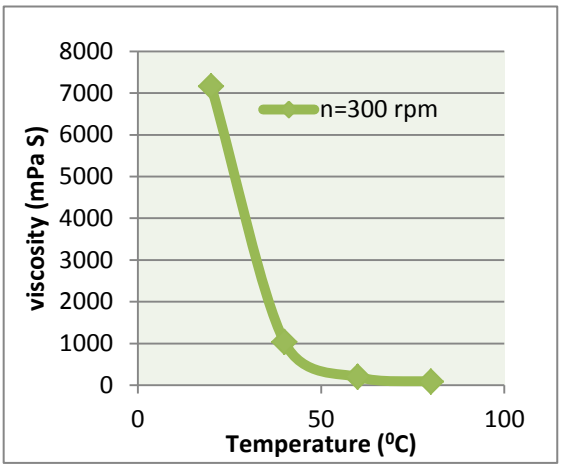

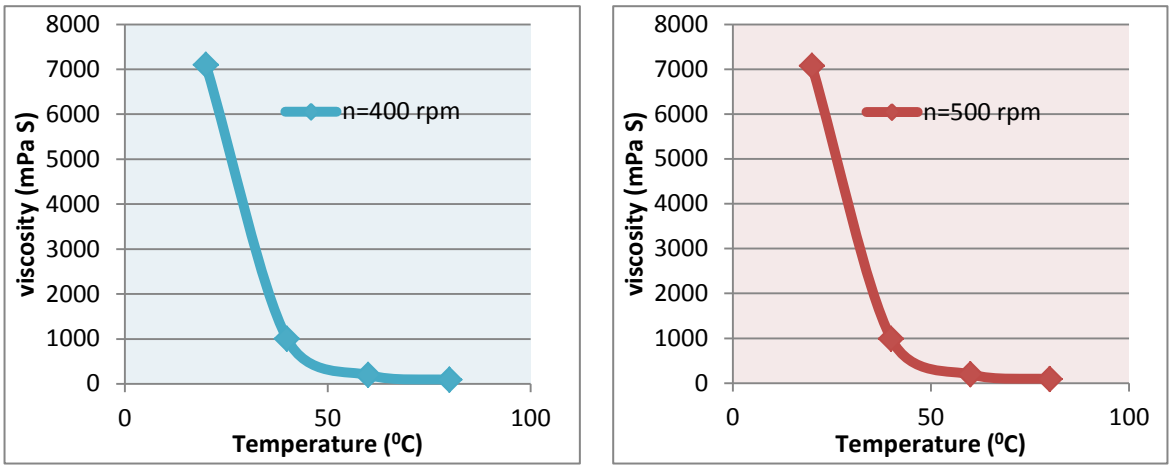

Figure 5. 5: The effect of temperature on viscosity at different shear rates.

Although the increase of shear rate has less impact on the changes of viscosity, its contribution on the reduction of viscosity should not be taken lightly especially in the case where bio-oils are applied in extremely high shear rate condition. Similar to the effect of temperature, the applied shear rate is used to break down the internal structure within the bio-oil very rapidly by reducing attraction forces between molecules. It also causes molecular interchange. This sheared energy is mostly absorbed by molecules of bio-oil that are closer to the moving part of any equipment, and this is differed from the energy provided by temperature, where the heat energy is spread all over the content of bio-oil. Therefore, this explains why the effect of temperature is more significant than shear rate, in the reduction of viscosity. The shear rate-viscosity profile is clearly presented in figure 5.6.

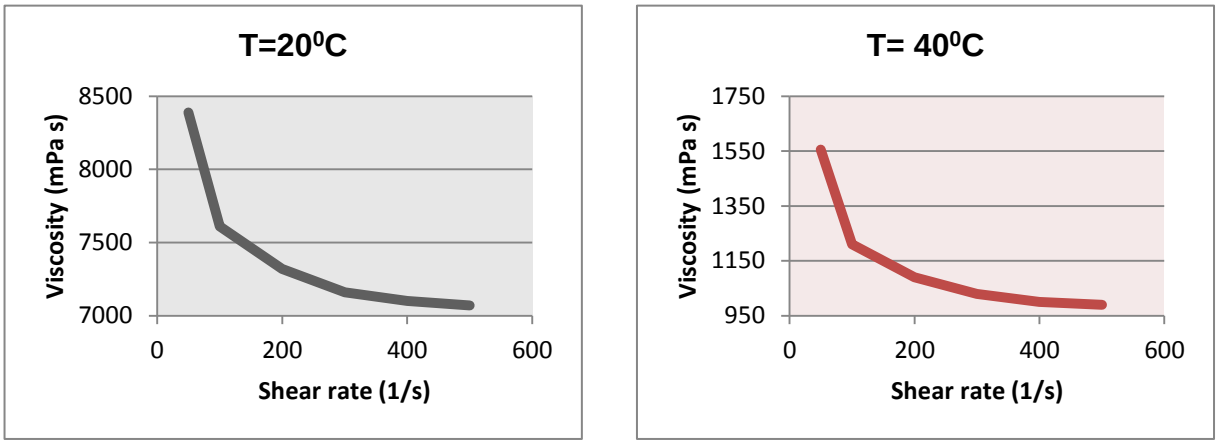

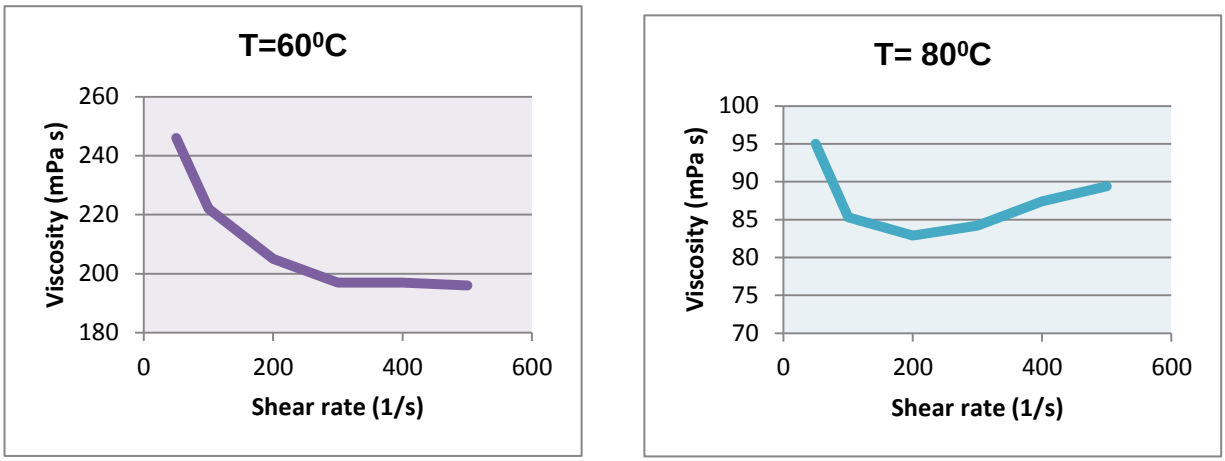

Figure 5. 6: The effect of shear rate on viscosity at different temperatures.

5.2 Model 2: viscosity at different solid mass fraction:

Solid content is one of the key parameter to describe the viscosity of organic condensate because when the percentage of solid in the sample is increased, the viscosity is increases, and up to certain range the solid content can be allowed in the organic condensate as shown in the figures 5.7 and 5.9. The range of solid content for these experiments is assumed to be 14%, higher range can be considered but more deviation is observed at higher solid contents. Experiments at 60 and 80^{0}C shows that the Viscosity gradually increases and it follows exponential behavior when the solid contents rise more than 12% as shown in the figure 5.7 and 5.9. The increase of viscosity with the addition of solid contents is due to the resistance to flow of organic condensate. The frictional effect increases and mobility of organic condensate is affected by the addition of solids in sampled fluid 2014-1313. When the frictional affect increases, due to solids, the motion of flowing liquid is hindered by these particles of solids. The size and distribution of particles and homogeneity of solids with sample fluid is important in motion of any fluid. Smaller the particle size better is the distribution of particles and this will give us smooth increase of viscosity. It is cleared from figures 5.7b and 5.9b that viscosity will increase, which is true generally, so better is homogeneity provides better results and same is for particle size distribution. As temperature has its own effect, when temperature increases, percentage of water and volatiles, which are already present in the sample, were evaporated. The evaporation of volatiles and water, at higher temperatures is high. So when temperature increases, evaporation will increase and it will give more solids as shown in Appendix 1. The solid contents, which were added externally and those, which were obtained through evaporation at higher temperatures, are responsible for the increase of dynamic viscosity of sampled fluid 2014-1313 as shown in Appendix 1.

Viscosity increases with the increase in particle concentration. Bio-oil with 14 % concentration has the higher viscosity and the 10% concentration the lower, within the range studied. The viscosity increases because the frictional forces between the particles becomes significant, and also because the blockage of

organic condensate occurs during flow. When the solid particles are added in organic condensate sample, it makes agglomeration and the concentration of this agglomeration increases as we add and more solid particles in sample. So, due to this reason the viscosity shows exponentially increasing trend in figures 5.7 and 5.9.

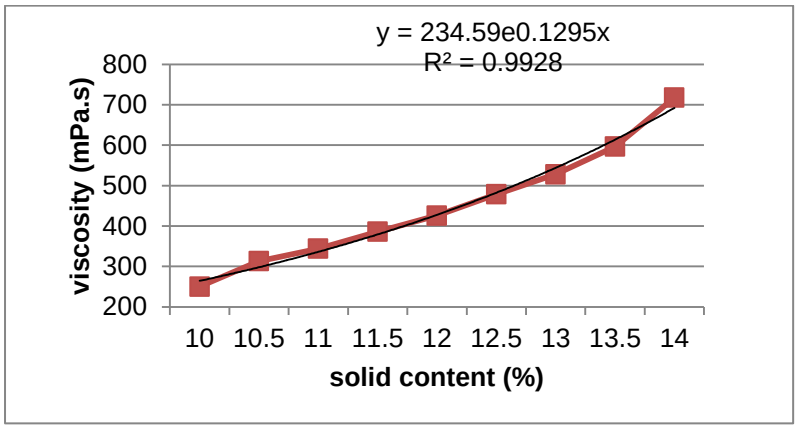

Figure 5.7: Dynamic viscosity at different solid Content wt. % at 60 ^{0}C

At 60^{0}C, the model which we get from graph is represented below:

$$\mathbf{y = 234.59e^{0.1295x}}$$

$$\mathbf{R^2 = 0.9928}$$

This model is valid in between the values of solid content from 10 to 14 wt. %. The maximum relative value of standard deviation experimentally concluded is 16%, which is at 13% of solid content. The value varies from 0.22 to 16 % and the range of solid content is 10 to 14 %. . Mean values of viscosity with confidence interval of 95% have been plotted by using Predint function of MATLAB as shown in the figure 5.7.

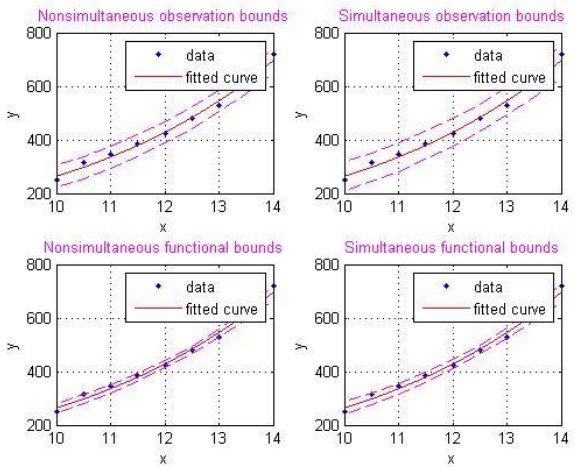

Figure 5.8: Confidence interval of 95% with solid content at 60 ºC

Table 5.2: Upper and Lower bound variations

	P1=	P2=	P3=	P4=	P5=	P6=	P7=	P8=	P9=
Points	250.1	313.2	344	386.1	426	478	527	596	717.4
Upper bound	740.455	657.07	584.86	522.04	467.05	418.68	375.95	338.095	304.49
Lower bound	648.24	572.97	504.64	443	387.73	338.44	294.67	255.91	221.65

So the whole model of solid contents at 60^0C is valid between these values because these are detected by confidence interval of 95%.

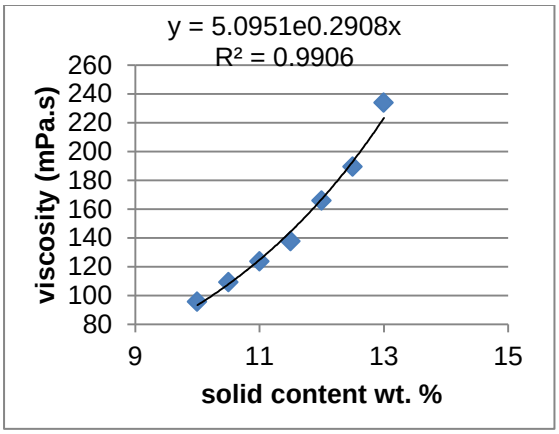

Figure 5.9: Dynamic viscosity at different solid Content wt. % at 80 ^{0}C

At 80^{0}C, the model which we get from graph is represented below:

$$y = 5.0951e^{0.2908x}$$

$$R^2 = 0.9906$$

This model is between the values of solid content from 10 to 13 wt. %. The relative value of standard deviation is 7%.

At 80^{0}C the viscosity is low in the range of 100 to 250 mPa s but at 60 ^{0}C the viscosity is high in the range of 200 to 700mPa.s, this effect is due to temperature as we have explained in previous model. Mean values of viscosity with confidence interval of 95% has been plotted by using Predint function of MATLAB as shown in the figure 5.9.

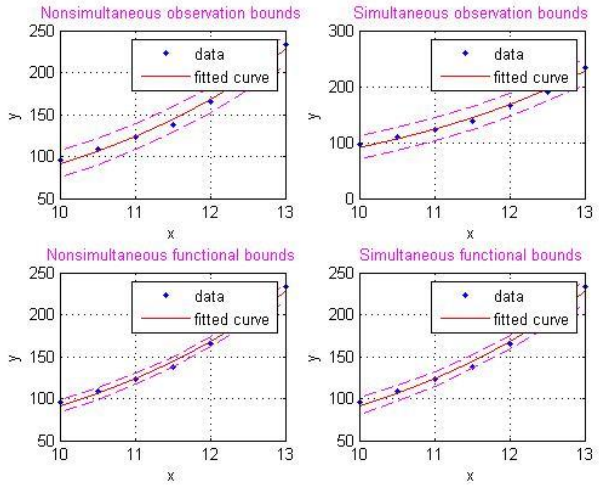

Figure 5.10: Confidence interval of 95% with solid content at 80^{0}C

Table 5.3: Upper and Lower bound variations

Points (x values)	P1=95.74	P2=109.3	P3=123.73	P4=137.8	P5=164	P6=189.4	P7=234
Upper bound(Y+)	245.2	211.03	182.76	159.1	139.05	121.91	107.91
Lower bound(Y-)	209.4	179.33	152.43	128.71	108.08	90.3	75

When we extrapolate the models from above mentioned equations both for 60 and 80 ^{0}C, the results are shown below:

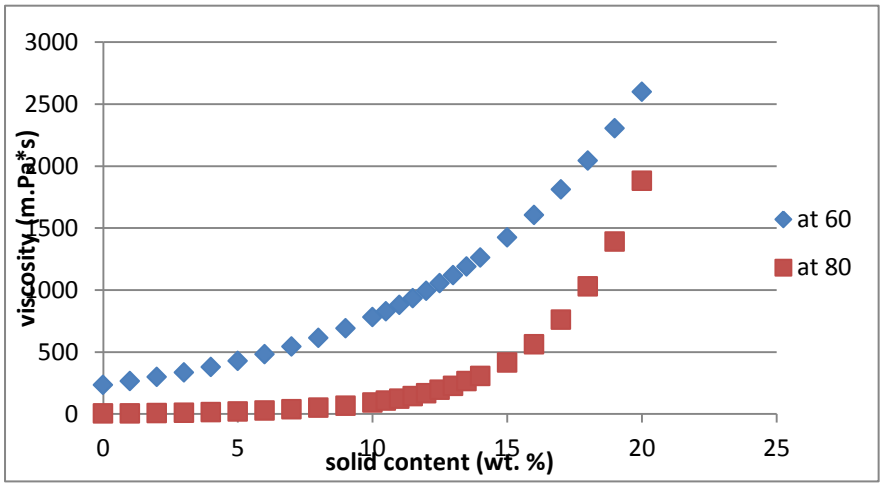

Figure 5.11: Extrapolation effect of model for 60 and 80^{0}C

The purpose of extrapolation is to show the trend line behavior of experimentally obtained exponential model. For example by micro filtration or other filtration techniques, if solid particles are removed from the sample 2014-1313 (organic condensate liquid) then the trend is shown in figure 5.11. These models can be compared with Krieger Dougherty model only when the solid particles are converted from mass fraction to volume fraction. The trend line for Krieger Dougherty is same with the model as shown in the figure 5.7 and 5.9. There are different models which explain the behaviour of solid content and viscosity. The best suitable is Krieger Dougherty because it is more similar to the developed models as the developed models as shown in figure 5.7 and 5.9. The main reason to choose Krieger Dougherty is the percentage of solid content which is higher than 10% and the curve fitting which has similarity with the developed models. The Different models curves are elaborated in chapter 3 in details.

It is important to analyze the effect that how much Percentage of solid contents are allowed in bio-oil because the solids present in the bio-oil may contain condensed carbon residual material, sand and metals. The inorganic solid content generally has several negative effects on bio-oil as a fuel. For

example, particles can agglomerate during storage and form a sludge layer on the bottom of the container, as well as facilitating the ageing of the oil, erosion in the pumps, and are problematical both in atomizing nozzles due to their erosion and clogging potential, and in combustion devices, where they can be deposited on hot surfaces and cause corrosion, as well as increase particulate emissions. When considering the areas of bio-oil handling, storage, stability, atomization quality and combustion behaviour, the presence of char is not desirable and low char oils should be favoured. From experiments, it is observed that solid contents higher than 14% shows higher change in viscosity, so the range of solid content at different temperatures is different as shown in figures 5.7 and 5.9.

5.3 Model 3: viscosity at different water mass fraction:

In fast pyrolysis bio-oils, the amount of water in bio fuels is regulated because it forms a separate phase that can cause corrosion, emulsion formation and problems in burners. Water is either dissolved or it exists as a microemulsions. It cannot be removed by physical methods such as centrifugation. Normally, the water content of the bio-oils is high, and it needs to be regulated because of its influence on other bio-oil properties as well as its influence on the phase stability.

The developed model obtained from the measurements through experiments is shown in the figure 5.13. The scale used here is logarithmic scale and the fitting accuracy of the model from Microsoft Excel and MATLAB is polynomial fit [59]. For comparison to Oasmaa's model, 5.13b model is used and the vertical axis is dynamic viscosity with base 10 and horizontal axis is water mass fraction with base 2 as shown in figure 5.13b. One important thing is that viscosity measurement is carried out at constant temperature of 40^0C. Fast pyrolysis bio-oils contain low-boiling (below 100°C) and water-soluble compound. This temperature is an intermediate temperature where the viscosity of bio-oil is not so much high and also the effects of temperature is not so much dominant like loss of volatiles and water is less. It can also be observed through analytical analysis of sample which was experimented with different percentage of water and after that it was tested in KIT analytical lab to make sure the original percentage of water in the sample and the results are mentioned in the appendix 2. There are number of parameters which effect analysis of viscosity with mass percentage of water such as density, heating values and phase stability of organic condensate.

The model with curve fitting is shown in figure 5.13 has an equation with standard deviation of 5% relatively:

$$\mathbf{y = -19.832x^2 + 390.32x - 3.4818}$$

$$\mathbf{R^2 = 0.9936}$$

Mean values of viscosity with confidence interval of 95% has been plotted by using Predint function of MATLAB as shown in the figure 5.12.

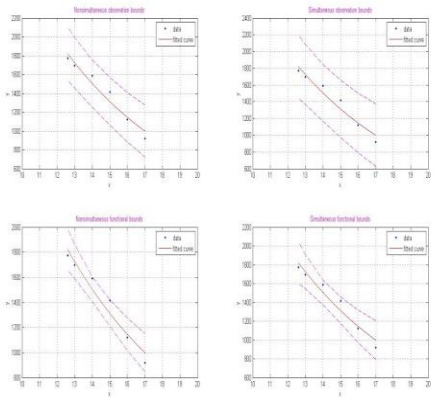

a)

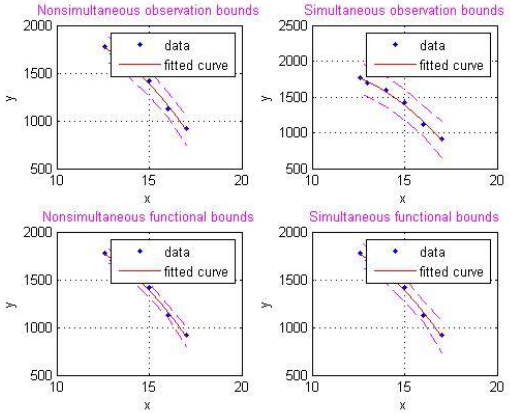

b)

Figure 5.12: a) Confidence interval of 95% with water content and exponential fit b) Confidence interval of 95% with water content and polynomial fitting

The better fitting is 5.12b that is polynomial fitting and is decreasing downward. The variation of points is given in the table 5.4 which defines the accuracy of the whole model through confidence interval of 95%.

Table 5.4: Upper and Lower bound variations

Points (x values)	P6=918.6	P5=1120	P4=1413.6	P3=1590.4	P2=1698	P1=1773.2
Upper bounds (Y+)	1052.9	1293.8	1523.3	1704.41	1848.9	1909
Lower bounds (Y-)	748.4	1035.7	1255.1	1443.9	1589.3	1623.2

So the whole model is valid in between in these values because these are detected by confidence interval of 95%.

It can be observed in the model that viscosity decreases when the water is added. The increase in water content improves the stability of the bio-oil until it starts to separate out, typically at above 30 wt% water content [59]. However, in case of wheat straw, we observed the phase separation approximately when 17% water content is achieved.

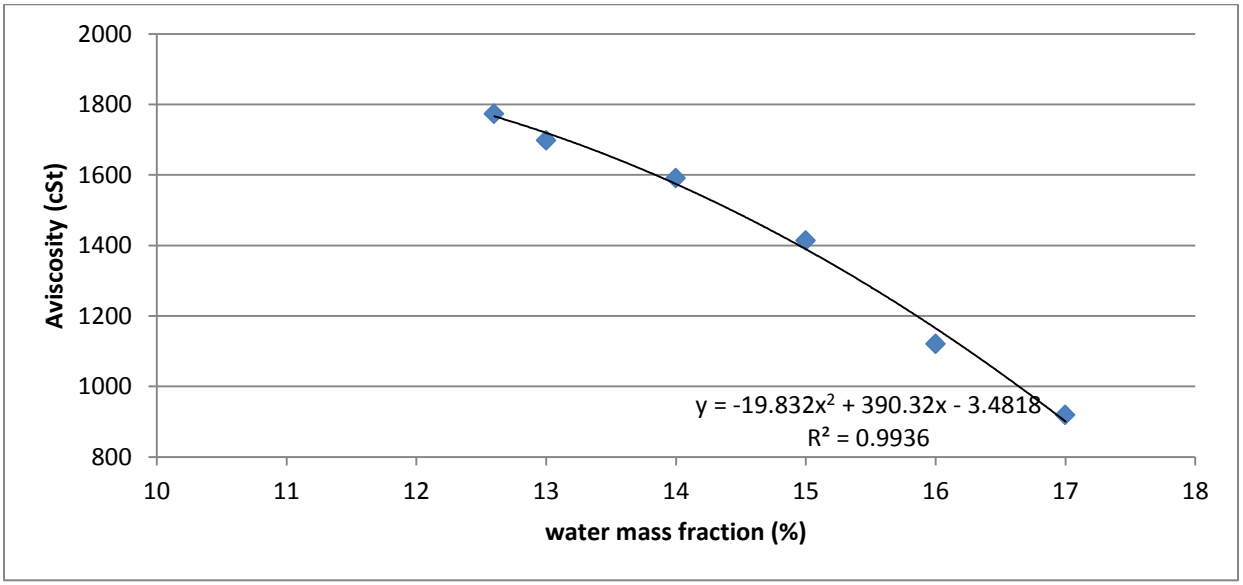

Figure 5.13 a: Viscosity of pyrolysis bio-oil from wheat straw as a function of water content.

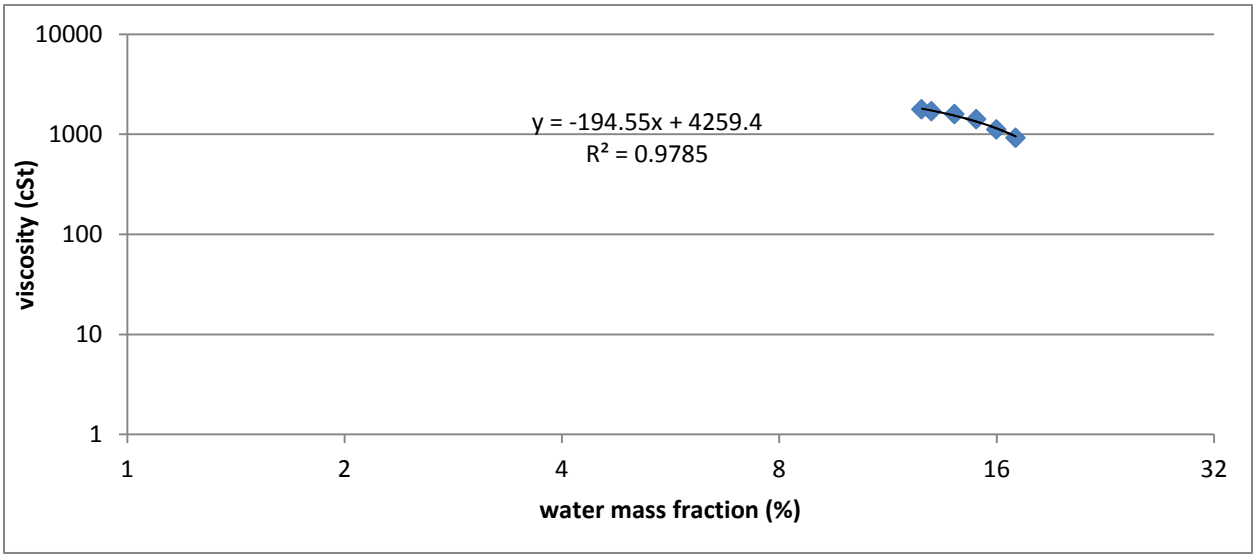

Figure 5.14 b: Viscosity of bio-oil from wheat straw as a function of water content on logrithmic scale.

This model can be compared with Oasmaa's model which has given for pine and forest residue as shown in the figure 5.14. Oasmaa studied the influence of water content on viscosity extensively for different biomass feedstocks which is more important to be understood in order to compare the trend developed for wheat straw with different water content. The range of water content is more dependent on the nature of the feedstock considered, in the case of wheat straw consumed in bioliq pilot plant, the feed stock was found to have a water content of around 20%.

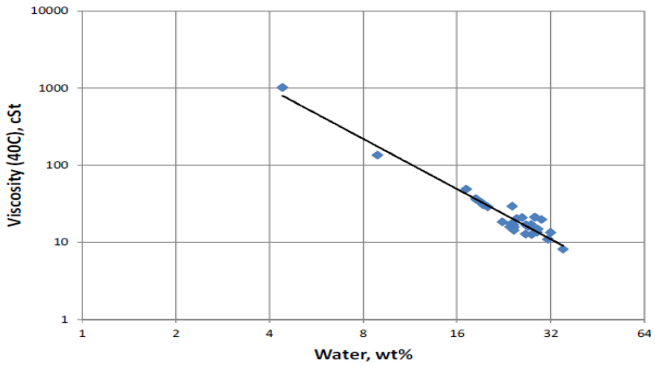

Figure 5.15: Viscosity of pyrolysis bio-oils from pine and forest residue as a function of water content [59].

The basic information conveyed by Oasmaa's model is that all kinds of bio-oil showed decrease in viscosity when water content is increased. This is physically explainable by change in surface tension and density due to the micro-emulsion of water. In order to investigate the same analysis here, the range of dynamic viscosity with water content is studied and plotted as shown in figure 5.13a&b.

The model developed by Oasmaa (considered kinematic viscosity) and current developed model (used dynamic viscosity) shows the similar analogous trend. This leads to the conclusion that the density variation has less or no effect and surface tension has to play the major factor of dependency for the comparison of viscosity.

Pyrolysis liquids such as bio-oil are a solution of organic compounds, high molecular weight lignin compounds exist as microemulsions. If the water content exceeds saturation level, the acids required to keep the lignin in solution are thought to be removed from around the lignin, the solubility balance of the pyrolysis liquid matrix changes [60]. This type of liquid is of poor quality and cannot be used as a fuel. As it is already mentioned that phase separation of wheat straw bio-oil was observed at 17 wt% and it is due to significant polarity, solubility, and density difference of extractives, and it also achieved increase in temperature and storage time. As our model shows that viscosity decreases when water content increases so it is due to melting of long-chain fatty acids and/or Alcohols [60]. At certain water wt. % in bio-oil phase stability is maintained which is advantageous but has negative effect on the quality of fuel as well. When phase separation takes place top phase consist of lower denser liquid such as water and bottom phase is of high density organic condensate. So the viscosity of bottom phase is higher than top

phase. It was observed during experiments that the phase separation is visible at higher temperatures; lower temperatures had to be used in order to reach good phase stability.

Negative effects of higher percentage of water by weight in different fields of applications are: the high water content of the bio-oil supply low energy density lowers the adiabatic flame temperature and local combustion temperatures as well as the combustion reaction rates. High wt. % of water content also causes difficulties in ignition and increases the ignition delay time by reducing the vaporization rate of the droplet, which causes problems in compression ignition engine applications.

Certain limitation of water presence as in our case 17 wt. % increases the atomization properties of the bio-oil by reducing its viscosity. It also decreases the thermal NOX-emissions by lowering the flame and local temperatures inside the combustor. However, too high water content in bio-oil may put at risk, the flame stability and controllability of the combustion, which might lead to higher total emissions of unburned particles [59, [60].

Heat transfer drop in Tar and Glycol:

The Nusselt number for flow inside a circular pipe for laminar flow is calculated by the following formula:

$$Nu = \left(3.66^3 + \left(1.62 + 0.293(Re * \frac{d}{l}) \right) \left(Re * Pr * \frac{d}{l} \right) \right)^{\frac{1}{3}}$$

The Nusselt number is calculated for glycol and organic condensate sample 2014-1313 by substituting the physical parameters of the above formula. To quantitatively investigate the viscosity dependence on heat transfer is done as follows: the Nusselt number is calculated by varying the viscosity from 2 to 30 centi-poise and plotted for both glycol and organic condensate. The selected range of viscosity for investigation is chosen by the operational temperature of heat exchangers. The operational temperature was 96^0C on which viscosity for glycol and organic condensate was determined and the range was selected. From the figures 5.15, as the viscosity of the fluid varies the heat transfer characteristics explained by the Nusselt number reduces. This might be able to explain that if the liquid used in the heat exchanger has higher viscosity then the heat transfer is predominantly affected but there is no prominent effect was found after changing the viscosity of the two fluids. The investigation of heat exchanger is co-related with model 1 because the operating temperature (i.e. 96^0C) viscosity was determined by the developed model 1.

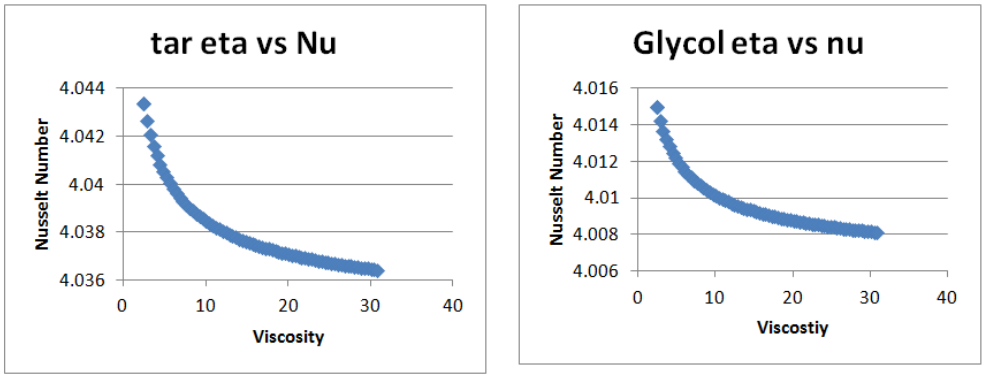

Figure 5.16: Behaviour of Viscosity with Nusselt number

When the viscosity of the liquid is increased, development of thermal and hydrodynamic boundary layer will also increase which eventually leads to the decrease in heat transfer coefficient this is illustrated in the following figure 5.16.

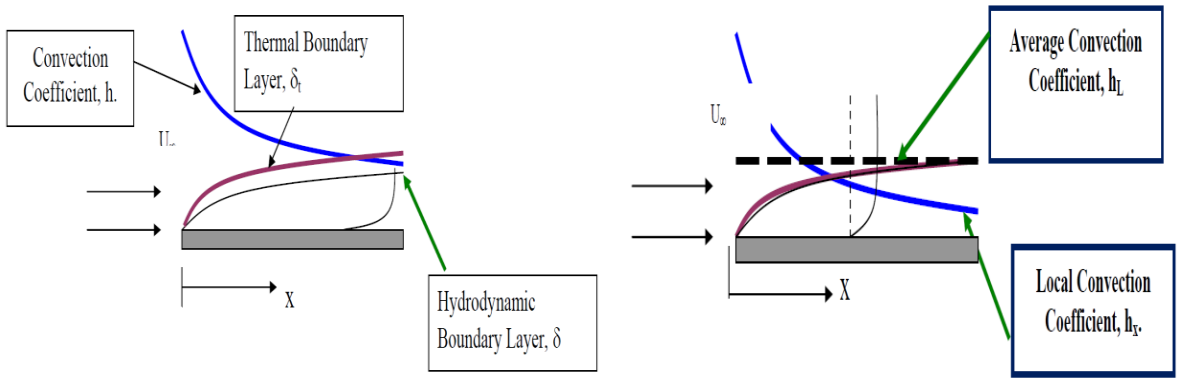

Figure 5.17: Boundry layer effect [84]

Eventually in most of the heat exchanger design, the average correlation is used so the effect of boundary layer has no influence formulating the average heat transfer coefficient so for the designing of the heat exchangers when it comes the predominantly viscous liquid like tar/organic condensate the local heat transfer correlations has to be taken into account for the design.

Chapter 6: Conclusions and Recommendations

The Experimental determination of viscosity for organic condensate is carried out and the model is developed for the temperature dependent viscosity. To test the technical feasibility of the organic condensate cycle, the variation of the temperature, solid content in tar and the water content in tar is studied. From the above discussed results it can be concluded that the model 1 gives accurate results and it proves the Arrhenius model is well adapted for the organic condensate. Other model developed (model 2&3) have a high confidence interval due to negligence of important factors such as the volume fraction and to avoid from evaporation. The density variation and boundary layer thickness are also negligible in heat exchanger calculations.

The variation of the mixture properties such as the solid and water mass fraction is studied. It was concluded that viscosity has exponential increase with increase of solid contents. In case of water content, viscosity decrease was observed and at higher temperatures evaporation effect was also determined that is proved by analytical lab as mentioned in appendix 2.

The investigation of the previous used heat exchangers network is studied by model 1 (i.e. the model of viscosity and temperature). The laminar flow inside a pipe condition is used to calculate the heat transfer characteristics. The heat transfer characteristics dependence on viscosity is formulated and major factor influencing the reduction in performance of heat exchanger can be interpreted from the Nusselt number dependence on viscosity.

The major factor which influences the heat exchanger performance is studied from the rheology point of view in this whole report but in practical case the exchanger performance is more dependent on the heat exchanger physical dimensions and the fouling resistance determined by the manufacturer’s data sheet. By studying the organic condensate physical properties, the heat exchanger used has to be adapted to the rheological properties and the pressure drop of the condensate.

Recommendation:

There are some suggestions related to future prospectus:

To avoid the evaporration of volatiles system should be modified little bit. It can be done by covering the rheometer with a flexibe disc or silver paper so that system act a closed system. In this way, evaporation can be reduced. For the determination of the viscosity of bio-oil samples always a new sample to fill in the measuring beaker. The main reason is this at higher temperatures evaporation and evaporation effects occurs, which can lead to incorrect viscosity values due to turbulent flow regimes.

It can be possible to calculate threshold point of solid contents for helical and cylindrical spindles geometries so accuracy in sense of solid content or water content can be clearly defined. From this study, it was concluded that 14 % solid content doesn't make so much difference in the viscosities of sampled fluid,with helical spindle same can be done with cylindrical difference and check the results. So, in this way we can define the threshold points for solid as well as water contents. It can be possible to measure the maximum packing fraction of sampled fluid 2014-1313 with some experiments or it can be assumed. It will be possible to compare exactly Kreiger Dougherty model or other regression models available in manuscripts, if mass percentage of solid contents of these experiments is converted to volume fraction.

References:

[1]. Directive on promotion of the use of energy from renewable, Official Journal of European Union vol.1. 140, pp. 16-62, 2009

[2]. Key world energy statistics of total supply of primary energy to the whole world. International energy agency, pp 6, 2013:

http://www.iea.org/publications/freepublications/publication/KeyWorld2013.pdf

[3].Federal Ministry for the Environment, Nature Conservation, and Nuclear Safety Construction, BMU-Bioenergy: Short survey for biomass utilization in Deutschland 2014.

http://www.erneuerbare-energien.de/die-themen/bioenergie/kurzinfol

[4]. Energy Information Administration (EIA), 2008

http://tonto.eia.doe.gov/energyexplained/index.cfm

[5]. A. Demirbas, Competitive liquid bio-fuels from biomass, pp. 17–28, 2011.

[6].E.Sadeghinezhad, S.N. Kaz, Foad Sadeghinejad, A. Badar-u-din, Mohammad Mehrali, Rad Sadri, Mohammad Reza Safaei, A comprehensive literature review of bio-fuel performance in internal combustion engine and relevant costs involvement Volume 30, February 2014, Pages 29–44, 2014.

[7]. Arifa sultana, Amit kumar, Development of tortuosity factor for assessment of lignocellulosic biomass delivery cost to a biorefinery ; Volume 119, 15 April 2014, Pages 288–295, 2014

[8]. Dahmen, Nicolas, Dinjus, Eckhard and Henrich, Edmund, Synthesis fuels from biomass, The Karlsruhe method bioliq - pp.59-63 2007b.

[9]. Federal Ministry for the Environment, Nature Conservation, and Nuclear Safety, BMU bioenergy: Short survey for biomass use in Germany, 2014.

http://www.erneuerbare-energiein.de/die-themen/bioenergie/kurzinfo/.

[10]. Dahmen N., Dinjus E., Kolb D., Arnold U., Leibold H. & Stahl R., state of the art of bioliq® process for synthetic biofuels production, Environmental progress & Sustainable Energy vol.31, No.2 176-181, 2012a.

[11]. Raffelt K., Henrich E., Koegel A., Stahl R., Steinhardt J. & Weirich F., The BTL2 process of biomass utilization entrained-flow gasification of pyrolyzed biomass slurries, Applied Biochemistry and Biotechnology, 153, 129-132, 2006

[12]. Bridgewater A.V & Peacocke G.V.C, Fast pyrolysis processes for biomass: Renewable and Sustainable Energy Reviews 4, 1-736, 2000.

[13a]. Gulben Erbay, Optimization of mixing process for the production of the bioliq® syncrude®: Master thesis in IKFT 2013

[13b]. Dahmen N., Die Schnellpyrolyse im Rahmen des bioliq®- Verfahrens am Forschungszentrum Karlsruhe. Gulzower Fachgesprache, Band 28, 2007.

[14]. Dahmen N., Henrich E., Dinjus E. & Weirich F., The bioliq® bioslurry gasification process for the production of biosynthetic fuels, organic chemicals and energy, Energy, Sustainability and society, 2:3, 2012b.

[15]. DAHMEN N. & DINJUS E., bioliq process concept, technology and state of development. MTZ Vol.71, 2010b

[16]. E. Henrich, N. Dahmen, K. Raffelt, R. Stahl, F. Weirich., The Karlsruhe "Bioliq" process for biomass gasification, Forschungszentrum Karlsruhe, 2007.

[17]. Henrich, E., Dinjus E., Das FZK-Konzept zur Kraftstoffherstelung aus Biomasse-Vergasung, Internationale Tagung, Leipzig, p.5, 2003.

[18]. Lynd, L. R., van Zyl, W. H., McBride, J. E., & Laser, M., Consolidated bio-processing of cellulosic biomass:. Current Opinion Biotechnology 16, 577–583, 0958-1669, 2005

[19]. Wornat, M. J., Porter, B. J., & Yang, N. Y., Single droplet combustion of biomass pyrolysis oils, Energy& Fuels 8, 1131–1142, 0887-0624, 1994.

[20]. Bridgewater, A. V., Biomass fast pyrolysis, Thermal Science 8(2), 21–49, 0354-9836, 2004.

[21]. C.Molgaard. Environmental impacts by disposal of plastic from municipal solid waste, Resour. Conserv. Recyc, vol, 15, no. 1, pp, 51-63, Oct, 1995

[22]. A. Bridgewater., “Renewable fuels and chemicals by thermal processing of biomass.” Chem. Eng. J., vol. 91, no. 2-3, pp.87-102, March 2003

[23]. A. V. Bridgewater, “Review of fast pyrolysis of biomass and product upgrading,” Biomass and Bioenergy, vol, 38, pp. 68-94., March 2012

[24]. Bridgewater, A. V., Renewable fuels and chemicals by thermal processing of biomass, Chemical Engineering Journal 91, *87–102,* 1385-8947, 200

[25]. Ringer, M., Putsche, V., & Scahill, J., Large-scale pyrolysis oil production: a technology assessment and economic analysis. NREL/TP-510-37779. National Renewable Energy Laboratory, Golden, Colorado, 2006

[26]. Diebold, J. P., & Czernik, S., Additives to lower and stabilize the viscosity of pyrolysis oils during storage, Energy & Fuels 11, 1081–1091, 0887-0624, 1997

[27]. Samolada, M. C., Papafotica, A., & Vasalos, I. A., Catalyst evaluation for catalytic biomass pyrolysis, Energy & Fuels 14, 1161–1167, 0887-0624, 2000

[28]. Lu, Q., Zhu, X-F., Li, W. Z., Zhang, Y., & Chen, D. Y., On-line catalytic upgrading of biomass fast pyrolysis products. Chinese Science Bulletin 54, 1941–1948, 1001-6538, 2009a

[29]. Tobias Bosch., product recovery options for fast pyrolysis of Lignocellulose, Master thesis in IKFT, 2012.

[30]. Branca, C. et al., multistep mechanism for the devolatilization of biomass fast pyrolysis oils, ind. Eng. Chem. Res. m 45, 5891-5899., 2006.

[31]. Bridgewater, A., Developments in Thermochemical biomass conversion, p. 402f, 1997

[32]. Oasmaa, A., MEIER, D., A.V. Bridgewater, H.Hofnauer, S. van Leo, norms and standards in thermal biomass conversion, epl-press, UK, p.79-93, 2009

[33]. Zhang Q., et al., reviews of biomass pyrolysis oil properties and upgrading research, energy conversion and management 48 p. 87-92, 2006

[34]. Bridgewater, A., et al., fast pyrolysis processes for biomass, renewable and sustainable energy reviews 4, p. 1-73, and p.61f, 2000

[35]. Ertas, M., & Alma, H., Pyrolysis of laurel (Laurus nobilis L.) extraction residues in a fixed-bed reactor: Characterization of bio-oil and bio-char. Journal of Analytical and Applied Pyrolysis 88, 22–29, 0165-2370, 2010

[36]. Onay, O., & Kockar, O. M., Pyrolysis of rape seed in a free fall reactor for production of bio-oil Fuel 85, 1921–1928, 0016-2361, 2006

[37]. Parihar, M. F., Kamil, M., Goyal, H. B., Gupta, A. K., & Bhatnagar, A. K., An experimental study on pyrolysis of biomass Trans ICheme, Part B, Process Safety and Environmental Protection 85(B5), 458–465, 0957-5820, 2007

[38]. Pootakham, T., & Kumar, A., Bio-oil transport by pipeline: A techno-economic assessment. Bioresource Technology 101, 7137–7143, 0960-8524, 2010a

[39]. Pootakham, T., & Kumar, A., A comparison of pipeline versus truck transport of bio-oil Bioresource Technology 101, 414–421, 0960 -8524, 2010b

[40]. Jones, D. S. J., & Pujadó, P. P., Handbook of Petroleum Processing, first Ed .Springer, Berlin Chapter 13, p. 545, 2006

[41]. Bridgewater, A. V., Principle and practice of biomass pyrolysis process for liquid. *Journal of* Analytical and Applied Pyrolysis 51, 3–22, 0165-2370, 1999

[42]. Thamburaj, R., Dynamotive engineering: Fast pyrolysis of biomass for green power generation http://www.dynamotive.com, 2000

[43]. Thangalazhy-Gopakumar, S., Adhikari, S., Ravindran, H., Gupta, R. B., Fasina, O., Tu, M., & Fernando, S. D., Physiochemical properties of bio-oil produced at various temperatures from pine wood using an auger reactor. Bioresource Technology 101(21), 8389-8395, 0960-8524, 2010

[44]. Ji-Lu, Z., Pyrolysis oil from fast pyrolysis of maize stalk, Journal of Analytical and Applied Pyrolysis 83, 205–212, 0165-2370, 2008.

[45]. Özaktas, T., Cıgızoglu, K. B., & Karaosmanog˘lu, F., Alternative diesel fuel study on four different types of vegetable oils of Turkish origin: Energy Sources 19, 173–181, 0090-8312, 1997.

[46]. Garcia-Perez, M., Lappas, P., Hughes, P., Dell, L., Chaala, A., Kretschmer, D., & Roy, C., Evaporation and combustion characteristics of bio-oils obtained by vacuum pyrolysis of wood industry residues: IFRF combustion *J*. Article No 200601, 1562-479X, 2006.

[47]. Oasmaa, A., Peacocke, C., Gust, S., Meier, D., & McLellan, R., Norms and standards for pyrolysis liquids, End-user requirements and specifications. Energy & Fuels *A-I,* 0887-0624, 2005

[48]. Qiang, L., Xu-lai, Y., & Xi-Feng, Z., Analysis on chemical and physical properties of bio-oil pyrolyzed from rice husk. Journal of Analytical and Applied Pyrolysis 82, 191– 198, 0165-2370, 2008

[49]. Calabria, R., Chiariello, F., & Massoli, P., Combustion fundamentals of Pyrolysis oil based fuels, Experimental Thermal and Fluid Science 31, 413–420, 0894-1777., 2007

[50]. Sensöz, S., & Kaynar, I., Bio-oil production from soybean; fuel properties of bio-oil, Industrial Crops and Products 23, 99–105, 0926-6690, 2006

[51]. Garcia-Perez, M., Chaala, A., & Roy, C., Vacuum pyrolysis of sugarcane bagasse, Journal of Analytical and Applied Pyrolysis, 65, 111-136, 0165-2370, 2002

[52]. Diebold, J. P., A review of the chemical and physical mechanisms of the storage stability of fast pyrolysis bio-oils, In Bridgewater AV, Editor Fast pyrolysis of biomass: A handbook, vol. 2. UK: CPL Press. ISBN 1872691471, 2002

[53]. Paul, edward L., atiemo-obeng,victor A.and Kresta,suzanne M., Handbook of industrial mixing. Hoboken,new jersey: john Wiley & sons, 2004. 0-471-26919-0, 2004

[54]. Barnes, H. A., J. F. Hutton, and K. Walters., An Introduction to Rheology, Elsevier, New York, 1989.

[55]. Paul, edward L., atiemo-obeng,victor A.and Kresta,suzanne M., Handbook of industrial mixing. Hoboken,new jersey :john Wiley & sons, 2004. 0-471-26919-0, 2004

[56]. Elert Glenn "Viscosity" The Physics Hypertext book

http://hypertextbook.com/physics/matter/viscosity/

[57]. A.A. Zaman, Techniques in Rheological Measurements: Fundamentals and Applications, Instructional Module, NSF Engineering Research Center for Particle Science and Technology, University of Florida, Gainesville, 1998

[58]. Oasmaa, A., Leppämäki, E., Koponen, P., Levander, J. & Tapola, E., Physical characterization of biomass-based pyrolysis bio-oils, Application of standard fuel oil analyses. Espoo, VTT, VTT Publications 306. http://www.vtt.fi/inf/pdf/publications/1997/P306.pdf, 1997

[59]. Diebold, J.P., Milne, T., Czernik, S., Oasmaa, A., Bridgwater, A.V., Cuevas, A., Gust, S., Huffman, D. & Piskorz, J., Proposed specifications for various grades of pyrolysis oils. In: Bridgwater, A.V. & Boocock, D.G.B. (Eds.): Developments in Thermochemical Biomass Conversion, Banff, 20–24 May 1996. Glasgow: Blackie Academic & Professional. Vol. 1 Pp. 33–447, 1997

[60]. Jani Lehto, Anja Oasmaa, Yrjö Solantausta, Matti Kytö & David Chiaramonti, Fuel oil quality and combustion of fast pyrolysis bio-oils Espoo 2013. VTT Technology 87, 2013

[61]. Oasmaa, A. & Peacocke, C., A guide to physical property characterization of biomass-derived fast pyrolysis liquids: Espoo, VTT Energy. VTT Publications 450 65 p. + app. 34 p. ISBN 951-38-5878-2; 951-38-6365-4 http://www.vtt.fi/inf/pdf/publications/2001/P450.pdf, 2001

[62]. Qiang, L., Xu-lai, Y., & Xi-Feng, Z., Analysis on chemical and physical properties of bio-oil pyrolyzed from rice husk. Journal of Analytical and Applied Pyrolysis, Vol. 82, No. 2, pp. 191–198, 2008

[63]. Tzanetakis, T., Ashgriz, N., James, D.F. & Thomson, and M.J., Liquid Fuel Properties of a Hardwood-Derived Bio-oil Fraction. Energy & Fuels, Vol. 22, No. 4, pp. 2725–2733, 2008

[64]. J.P. Diebold, J. W. Scahill, S. Czernik, S.D. Phillips, C.J. Feik., progress in the production of hot gas filtered biocrude oil at NREL, 1995

[65]. Oasmaa, A., Kuoppala, E. & Solantausta, and Y., Fast pyrolysis of forestry residue. 2. Physicochemical composition of product liquid. Energy and fuels, Vol. 17, No. 2, pp. 433–443, 2003a

[66]. Oasmaa, A., Kuoppala, E., Solantausta, Y. & Gust, S., Fast pyrolysis of forestry residue: Effect of extractives on phase separation of pyrolysis bio-oils. Energy & Fuels, Vol. 17, No. 1, pp. 1–12, 2003b

[67]. Oasmaa, A., Kuoppala, E., Selin, J.-F., Gust, S. & Solantausta, Y., Fast Pyrolysis of Forestry Residue and Pine, Improvement of the Product Quality by Solvent Addition, Energy & Fuels, Vol. 18, No. 5, pp. 1578–1583, 2004

[68]. García-Pérez, M., Chaala, A., Pakdel, H., Kretschmer, D., Rodrigue, D. & Roy, C., Multiphase Structure of Bio-Oils, Energy Fuels, 20, pp. 364–375, 2006a

[69]. Oasmaa, A. & Peacocke, C., A guide to physical property characterization of biomass-derived fast pyrolysis liquids. A guide Espoo: VTT

VTT Publications 731, 2010. http://www.vtt.fi/inf/pdf/publications/2010/P731.pdf

[70]. Diebold, J. P: A Review of the Chemical and Physical Mechanisms of the Storage Stability of Fast Pyrolysis Bio-oils. In Fast Pyrolysis of Biomass: A Handbook; Bridgwater, A. V., Ed.; CPL Press: Newbury, U.K., 2002; Vol. 2.

[71]. Agblevor, F.A., Besler, S. & Evans R.J., Inorganic Compounds in Biomass Feedstocks: Their Role in Char Formation and Effect on the Quality of Fast Pyrolysis Oils. In: Proceedings, Biomass Pyrolysis Oil Properties and Combustion Meeting, September 26–28, Estes Park, Colorado. Milne, T. A. (Ed.). NREL-CP-430-7215, National Renewable Energy Laboratory, Golden, Colorado, Pp. 77–89, 1995

[72]. Nicolaus Dahmen**,** Edmund Henrich**,** Eckhard Dinjus and Friedhelm Weirich, The bioliq bioslurry gasification process for the production of Biosyncrude, organic chemicals and energy; Energy, Sustainability and Society 2012, 2**:**3, 2012

[73]. Oasmaa, A., Korhonen, J. & Kuoppala, E., An approach for stability measurement of wood-based fast pyrolysis bio-oils: ACS Publications. Energy & Fuels, Vol. 25, No. 7, pp. 3307–3313. Doi: 10.1021/ef2006673, 2011

[74]. Oasmaa, A Fuel Oil Quality Properties of Wood-Based Pyrolysis Liquids: Academic dissertation, Department of Chemistry, University of Jyväskylä, Finland, VTT Research Report Series, Report 99; ISBN 951-39-1572-7, 2003

[75]. Oasmaa, A.; Kuoppala, E. Fast Pyrolysis of Forestry Residue & Storage Stability of Liquid Fuel: Energy Fuels 2003, 1075− 1084.Peacocke 2003: Determination of norms and standards for biomass fast pyrolysis liquids as an alternative renewable fuel for electricity and heat production, Pyrolysis Final Report, Part 2, 2003.

[76]. Boris Bitsch, Master thesis: Rheological characterization of a model pyrolysis slurries based of glycol and straw, 2011

[77]. Joel Leroy, Lionel choplin and Serge Kaliaguine., Rheological characterization of pyrolytic wood derived oils, existence of a compensation effect, Department de genie chimique, Universite Laval, Quebec, QC, GIK 7P4, Canada, 1988

[78]. Sunny Goh Eng Giap: The Hidden Property of Arrhenius-type Relationship, Viscosity as a Function of Temperature, Department of Engineering Science, Faculty of Science and Technology, Universiti Malaysia Terengganu, Mengabang Telipot, 21030 Kuala Terengganu, Terengganu, Malaysia, 2010

[79]. McCabe, Warren L., Julian C. Smith and Peter Harriot: Unit operations of Chemical Engineering, 5th ed., New York, McGraw-Hill Book Company, 1993

[80]. Ramesh K. Shah and Dusan P. Sekulic: Fundamentals of heat exchanger design, ISBN 0-471-32171-0, John Wiley & Sons, Inc., Hoboken, New Jersey, 2003

[81]. Yunus A. Çengel: Heat Transfer, a Practical Approach (2nd Ed.). McGraw-Hill, 2003

[82]. Wenke / Buchberger: Rheological characterization of fluids with helical measuring systems, IKFT fuel analysis - Internal Project Report, 2012

[83]. Axel Funke: IFKT Research work on wheat straw, 2013

[84]. Volker Gnielinski: Heat transfer in a pipe flow, KIT, Karlsruhe, Germany.

Appendix

Appendix 1

Sample analysis after Solid addition at 60 and 80^{0}C:

Institute of Catalysis Research and Technology
Analytic
Fr. Heinrich

Karlsruhe institute of technology (KIT)
Hermann-von-Helmholtz-Platz 1
D-76344 Eggenstein-Leopoldshafen
Tel. 0721/608-26508

Date 16.09.2014

IKFT / Hr. judge order: 201459
Kd.Nr. 2428

Python

Sample name: **2014-1313 with water content Rizwan 10.09.** Analyse-Nr: **201427728**

Collection kit / origin: Python fast pyrolysis

Note on the sample: Datum:

16.09.2014

Sample of Rizwan

investigation results			
Analysis	Remark	Unit	Results
H2O-POT	16,26 / 16,37 / 16,43	%	16.4
solid		%	15.4

Institute of Catalysis Research and Technology
Analytic
Fr. Heinrich

Karlsruhe institute of technology (KIT)
Hermann-von-Helmholtz-Platz 1
D-76344 Eggenstein-Leopoldshafen
Tel. 0721/608-26508

Date 10.09.2014

IKFT / Hr. judge order: 201459
Kd.Nr. 2428

Python

Sample name: **2014-1313 with water content Rizwan 10.09.** Analyse-Nr: **20142779**

Collection kit / origin: Python fast pyrolysis

Note on the sample: Datum:

15.09.2014

Sample of Rizwan

investigation results			
Analysis	Remark	Unit	Results
H2O-POT	16,26 / 16,37 / 16,43	%	16.4
Solid		%	13.8

Appendix 2

Sample analysis after water addition:

Institute of Catalysis Research and Technology
Analytic
Fr. Heinrich

Karlsruhe institute of technology (KIT)
Hermann-von-Helmholtz-Platz 1
D-76344 Eggenstein-Leopoldshafen
Tel. 0721/608-26508

Date 10.09.2014

IKFT / Hr. judge

order: 201459

Kd.Nr. 2428

Python

Sample name: **2014-1313 with water content Rizwan 10.09.**

Analyse-Nr: **20142737**

Collection kit / origin: Python fast pyrolysis

Note on the sample:

Datum:

10.09.2014

Sample of Rizwan

investigation results			
Analysis	Remark	Unit	Results
H2O-POT	16,26 / 16,37 / 16,43	%	16,4
pH			4,3

Appendix 3

Calculation of water percentage:

$$\textbf{Mass Percentage of water} = \frac{\textbf{Mass of water already in sample} + \textbf{Mass of added water}}{\textbf{Mass of added water} + \textbf{Mass of Tar}}$$

For example:

Sample weight= 54 grams

Weight of beaker= 7.9 grams

Original weight = 54 - 7.9= 46.1 grams

Water already present in sample= 12.6 % of the original weight = 5.8 grams

From above Equation, if we are trying to find 13% of water of the total weight then, we need:

Mass of added water= 0.25 grams

Calculation of Solid Percentage:

$$\textbf{Mass percentage of solid} = \frac{\textbf{Mass of solid already in sample} + \textbf{Mass of added solid}}{\textbf{Mass of Tar} + \textbf{Mass of added solid}}$$

For example:

Sample weight= 54 grams

Weight of beaker= 7.9 grams

Original weight = 54 - 7.9= 46.1 grams

Solid already present in sample= 10 % of the original weight = 4.61 grams

From above Equation, if we are trying to find 11% of solids of the total weight then, we need:

Mass of added water= 0.5 grams

Appendix 4:

Modeling calculation and experimental values for Temperature, solid content and water mass fraction:

Model 1:

Temperatures	Viscosity					Mean value	absolute	relative	1/T (K^-1)	Log of viscosity
80 °C	93.9	92.83	93.8	96.61	93.7	94.168	1.430024	0.015167	3.412969	9.034557
60°C	250.3	246	249.9	237	245.4	245.72	5.354157	0.021783	3.194888	7.348845
40°C	1530	1580	1499	1608	1555	1554.4	42.40637	0.027284	3.003003	5.504518
20°C	8499	8182	8237	8672	8350	8388	199.7861	0.023791	2.832861	4.54508

Model 3:

water content	viscosity						absolute	relative
12.6	1742	1781	1781	1781	1781	1773.2	17.4413302	0.98360761
13	1690	1693	1691	1694	1722	1698	13.5092561	0.79559812
14	1595	1591	1613	1580	1573	1590.4	15.3557807	0.96552947
15	1409	1367	1524	1442	1326	1413.6	75.5996032	5.34801947
16	1086	1162	1094	1136	1122	1120	31.0483494	2.77217405
17	888	945	880	933	947	918.6	32.1605348	3.50103797

Model 2:

solid content(%age by wt) 60°C	viscosity		Mean	absolute	relative
	M-1	M-2			
10	250.3	249.9	250.1	0.282843	0.113092
10.5	316.5	309.9	313.2	4.666905	1.490072
11	349.2	338.8	344	7.353911	2.137765
11.5	389	383.2	386.1	4.101219	1.062217
12	430.8	421.2	426	6.788225	1.59348
12.5	483.5	473.4	478.45	7.141778	1.492691
13	541.8	513.9	527.85	19.72828	3.737478
13.5	613.5	579.5	596.5	24.04163	4.030449
14	736.3	698.5	717.4	26.72864	3.725765

solid content(%age by wt) 80°C	viscosity			Mean	absolute	relative
	M1	M2	M3			
10	96.61	96.61	94	95.74	1.506884	1.573934
10.5	103.8	111.9	112.4	109.3667	4.827353	4.413916
11	121.2	126.5	123.5	123.7333	2.657693	2.14792
11.5	132.8	143.4	137.2	137.8	5.325411	3.864594
12	153.8	179.9	164	165.9	13.15333	7.928467
12.5	187.7	200.5	180	189.4	10.35519	5.467366
13	235	250.8	216	233.9333	17.4245	7.448491

Appendix 5: Heat Transfer calculations:

Glycol	Glycol	Tar	Average/Mix	
Mass flow(Kg/h)	28780	34320	29000	8.05556
Area	3.58	3.58		
Diameter	0.0285			
Density	1062	1200		
Cp	2.03	2.5	2.265	
Thermal cond	0.2588	0.2588	0.2588	
Length	4	4		

Gylcol							
Eta	mas flow	vel	re	Pr	Re*Pr*d/L	1.62+0.293(RE*d/l)	Nu
2.3884	8.055555556	0.002118079	26.85036959	18.7344	3.584049219	4.379682892	4.015045319
2.4	8.055555556	0.002118079	26.7205928	18.8253	3.584049219	4.379372809	4.015022339
2.8	8.055555556	0.002118079	22.90336526	21.9629	3.584049219	4.369889294	4.014319392
3.2	8.055555556	0.002118079	20.0404446	25.1005	3.584049219	4.362244852	4.013752584
3.6	8.055555556	0.002118079	17.81372853	28.238	3.584049219	4.35591285	4.013282968
4	8.055555556	0.002118079	16.03235568	31.3756	3.584049219	4.350556163	4.0128856
4.4	8.055555556	0.002118079	14.57486888	34.5131	3.584049219	4.345947649	4.012543667
4.8	8.055555556	0.002118079	13.36029664	37.6507	3.584049219	4.341927931	4.012245379
5.2	8.055555556	0.002118079	12.33258129	40.7883	3.584049219	4.338381445	4.011982168
5.6	8.055555556	0.002118079	11.45168263	43.9258	3.584049219	4.335222074	4.011747658
6	8.055555556	0.002118079	10.68823712	47.0634	3.584049219	4.332384157	4.011536985
6.4	8.055555556	0.002118079	10.0202223	50.2009	3.584049219	4.329816637	4.011346367
6.8	8.055555556	0.002118079	9.430797459	53.3385	3.584049219	4.327479134	4.011172809
7.2	8.055555556	0.002118079	8.906864267	56.476	3.584049219	4.325339235	4.011013911
7.6	8.055555556	0.002118079	8.438081937	59.6136	3.584049219	4.323370581	4.010867716
8	8.055555556	0.002118079	8.0161778 4	62.7512	3.584049219	4.321551486	4.010732619
8.4	8.055555556	0.002118079	7.634455086	65.8887	3.584049219	4.319863925	4.010607282
8.8	8.055555556	0.002118079	7.2874344	69.0263	3.584049219	4.318292774	4.010490585

9.2	8.055555556	0.00211879	6.970589426	72.1638	3.584049219	4.316825237	4.010381577
9.6	8.055555556	0.00211879	6.6801482	75.3014	3.584049219	4.315450405	4.010279449
10	8.055555556	0.00211879	6.412942272	78.4389	3.584049219	4.31415891	4.010183508
10.4	8.055555556	0.00211879	6.166290646	81.5765	3.584049219	4.31294266	4.010093152
10.8	8.055555556	0.00211879	5.937909511	84.7141	3.584049219	4.311794621	4.010007859
11.2	8.055555556	0.00211879	5.725841314	87.8516	3.584049219	4.310708647	4.009927175
11.6	8.055555556	0.00211879	5.52839851	90.9892	3.584049219	4.30967934	4.009850698
12	8.055555556	0.00211879	5.344118556	94.1267	3.584049219	4.308701937	4.009778074
12.4	8.055555556	0.00211879	5.171727639	97.2643	3.584049219	4.307772217	4.009708991
12.8	8.055555556	0.00211879	5.010111115	100.402	3.584049219	4.306886426	4.00964317
13.2	8.055555556	0.00211879	4.8582896	103.539	3.584049219	4.30604121	4.009580362
13.6	8.055555556	0.00211879	4.715398729	106.677	3.584049219	4.305233562	4.009520343
14	8.055555556	0.00211879	4.580673051	109.815	3.584049219	4.30446078	4.009462914
14.4	8.055555556	0.00211879	4.453432133	112.952	3.584049219	4.303720425	4.009407894
14.8	8.055555556	0.00211879	4.333069103	116.09	3.584049219	4.303010291	4.009355117
15.2	8.055555556	0.00211879	4.219040968	119.227	3.584049219	4.302328376	4.009304437
15.6	8.055555556	0.00211879	4.110860431	122.365	3.584049219	4.30167286	4.009255718
16	8.055555556	0.00211879	4.008088902	125.502	3.584049219	4.301042082	4.009208835
16.4	8.055555556	0.00211879	3.910330654	128.64	3.584049219	4.300434524	4.009163678
16.8	8.055555556	0.00211879	3.817227543	131.777	3.584049219	4.299848796	4.009120142
17.2	8.055555556	0.00211879	3.728454809	134.915	3.584049219	4.299283621	4.009078133
17.6	8.055555556	0.00211879	3.6437172	138.053	3.584049219	4.298737825	4.009037564
18	8.055555556	0.00211879	3.562745707	141.19	3.584049219	4.298210324	4.008998354
18.4	8.055555556	0.00211879	3.485294713	144.328	3.584049219	4.297700119	4.008960428
18.8	8.055555556	0.00211879	3.411139506	147.465	3.584049219	4.297206286	4.008923719
19.2	8.055555556	0.00211879	3.3400741	150.603	3.584049219	4.296727966	4.008888163
19.6	8.055555556	0.00211879	3.271909322	153.74	3.584049219	4.296264364	4.0088537

20	8.055555556	0.002118079	3.206471136	156.878	3.584049219	4.295814741	4.008820275
20.4	8.055555556	0.002118079	3.143599153	160.015	3.584049219	4.295378408	4.008787838
20.8	8.055555556	0.002118079	3.083145323	163.153	3.584049219	4.294954722	4.008756341
21.2	8.055555556	0.002118079	3.02497277	166.291	3.584049219	4.294543085	4.008725739
21.6	8.055555556	0.002118079	2.968954756	169.428	3.584049219	4.294142936	4.00869599
22	8.055555556	0.002118079	2.914973776	172.566	3.584049219	4.293753751	4.008667056
22.4	8.055555556	0.002118079	2.862920657	175.703	3.584049219	4.293375037	4.008638901
22.8	8.055555556	0.002118079	2.812693979	178.841	3.584049219	4.293006333	4.008611489
23.2	8.055555556	0.002118079	2.764199255	181.978	3.584049219	4.292647207	4.008584789
23.6	8.055555556	0.002118079	2.717348442	185.116	3.584049219	4.29229725	4.00855877
24	8.055555556	0.002118079	2.672059228	188.253	3.584049219	4.291956078	4.008533404
24.4	8.055555556	0.002118079	2.628255029	191.391	3.584049219	4.291623331	4.008508664
24.8	8.055555556	0.002118079	2.585863819	194.529	3.584049219	4.291298667	4.008484525
25.2	8.055555556	0.002118079	2.544818362	197.666	3.584049219	4.290981765	4.008460962
25.6	8.055555556	0.002118079	2.505055575	200.804	3.584049219	4.290672319	4.008437954
26	8.055555556	0.002118079	2.466516258	203.941	3.584049219	4.290370041	4.008415478
26.4	8.055555556	0.002118079	2.4291448	207.079	3.584049219	4.29007466	4.008393515
26.8	8.055555556	0.002118079	2.392888907	210.216	3.584049219	4.289785917	4.008372046
27.2	8.055555556	0.002118079	2.357699365	213.354	3.584049219	4.289503567	4.008351051
27.6	8.055555556	0.002118079	2.323529809	216.491	3.584049219	4.289227377	4.008330514
28	8.055555556	0.002118079	2.290336526	219.629	3.584049219	4.288957128	4.008310419
28.4	8.055555556	0.002118079	2.258078265	222.767	3.584049219	4.288692607	4.00829075
28.8	8.055555556	0.002118079	2.226716067	225.904	3.584049219	4.288433617	4.008271491
29.2	8.055555556	0.002118079	2.196213107	229.042	3.584049219	4.288179968	4.00825263
29.6	8.055555556	0.002118079	2.166534551	232.179	3.584049219	4.287931477	4.008234152
30	8.055555556	0.002118079	2.137647424	235.317	3.584049219	4.287687973	4.008216044
30.4	8.055555556	0.002118079	2.109520484	238.454	3.584049219	4.28744929	4.008198296

30.8	8.055555556	0.00211879	2.082124114	241.592	3.584049219	4.287215273	4.008180893

Tar							
Eta	mas flow	vel	re	Pr	Re*Pr*d/L	1.62+0.293(RE*d/l)	Nu
2.3884	8.055555556	0.001875129	23.76257708	23.07187017	3.90626054	4.372089	4.043410811
2.4	8.055555556	0.001875129	23.64772463	23.18392581	3.90626054	4.371797	4.043387579
2.8	8.055555556	0.001875129	20.26947825	27.04791345	3.90626054	4.362876	4.042676911
3.2	8.055555556	0.001875129	17.73579347	30.91190108	3.90626054	4.355684	4.042103876
3.6	8.055555556	0.001875129	15.76514975	34.77588872	3.90626054	4.349727	4.0416291
4	8.055555556	0.001875129	14.18863478	38.63987635	3.90626054	4.344688	4.041227367
4.4	8.055555556	0.001875129	12.89875889	42.50386399	3.90626054	4.340353	4.0408816 8
4.8	8.055555556	0.001875129	11.82386231	46.36785162	3.90626054	4.336571	4.0405801 1
5.2	8.055555556	0.001875129	10.91433444	50.23183926	3.90626054	4.333235	4.040314007
5.6	8.055555556	0.001875129	10.13473913	54.09582689	3.90626054	4.330263	4.0400769 2
6	8.055555556	0.001875129	9.459089851	57.95981453	3.90626054	4.327593	4.039863932
6.4	8.055555556	0.001875129	8.867896735	61.82380216	3.90626054	4.325178	4.039671218
6.8	8.055555556	0.001875129	8.346255751	65.68778978	3.90626054	4.322979	4.039495753
7.2	8.055555556	0.001875129	7.882574876	69.55177743	3.90626054	4.320966	4.039335108
7.6	8.055555556	0.001875129	7.467702514	73.41576507	3.90626054	4.319114	4.039187307
8	8.055555556	0.001875129	7.094317388	77.279752 7	3.90626054	4.317402	4.039050725
8.4	8.055555556	0.001875129	6.756492751	81.14374034	3.90626054	4.315815	4.0389240 1
8.8	8.055555556	0.001875129	6.449379444	85.00772798	3.90626054	4.314337	4.0388060 3
9.2	8.055555556	0.001875129	6.168971642	88.87171561	3.90626054	4.312956	4.038695824
9.6	8.055555556	0.001875129	5.911931157	92.73570325	3.90626054	4.311663	4.038592573
10	8.055555556	0.001875129	5.675453911	96.59969088	3.90626054	4.310448	4.038495577
10.4	8.055555556	0.001875129	5.457167222	100.4636785	3.90626054	4.309303	4.038404228
10.8	8.055555556	0.001875129	5.255049917	104.3276662	3.90626054	4.308223	4.038317998
11.2	8.055555556	0.001875129	5.067369563	108.1916538	3.90626054	4.307202	4.038236427
11.6	8.055555556	0.001875129	4.892632682	112.0556414	3.90626054	4.306234	4.038159108
12	8.0555555	0.0018751	4.7295449	115.91962	3.906260	4.305314	4.0380856

	56	29	26	91	54		86
12.4	8.055555556	0.001875129	4.57697896	119.7836167	3.90626054	4.304439	4.038015844
12.8	8.055555556	0.001875129	4.433948368	123.6476043	3.90626054	4.303606	4.037949299
13.2	8.055555556	0.001875129	4.299586296	127.511592	3.90626054	4.302811	4.037885822
13.6	8.055555556	0.001875129	4.173127875	131.3755796	3.90626054	4.302051	4.037825122
14	8.055555556	0.001875129	4.053895665	135.2395672	3.90626054	4.301324	4.037767062
14.4	8.055555556	0.001875129	3.941287438	139.1035549	3.90626054	4.300628	4.037711436
14.8	8.055555556	0.001875129	3.834766156	142.9675425	3.90626054	4.29996	4.03765808
15.2	8.055555556	0.001875129	3.733851257	146.8315301	3.90626054	4.299318	4.037606842
15.6	8.055555556	0.001875129	3.638111481	150.6955178	3.90626054	4.298701	4.037557587
16	8.055555556	0.001875129	3.547158694	154.5595054	3.90626054	4.298108	4.03751019
16.4	8.055555556	0.001875129	3.460642628	158.423493	3.90626054	4.297537	4.037464536
16.8	8.055555556	0.001875129	3.378246375	162.2874807	3.90626054	4.296986	4.037420521
17.2	8.055555556	0.001875129	3.299682506	166.1514683	3.90626054	4.296454	4.03737805
17.6	8.055555556	0.001875129	3.224689722	170.015456	3.90626054	4.29594	4.037337035
18	8.055555556	0.001875129	3.153029955	173.8794436	3.90626054	4.295444	4.037297394
18.4	8.055555556	0.001875129	3.084485821	177.7434312	3.90626054	4.294964	4.037259051
18.8	8.055555556	0.001875129	3.018858463	181.6074189	3.90626054	4.2945	4.037221939
19.2	8.055555556	0.001875129	2.955965578	185.4714065	3.90626054	4.29405	4.037185991
19.6	8.055555556	0.001875129	2.895639705	189.3353941	3.90626054	4.293613	4.037151149
20	8.055555556	0.001875129	2.837726955	193.1993818	3.90626054	4.293191	4.037117357
20.4	8.055555556	0.001875129	2.782085225	197.0633694	3.90626054	4.29278	4.037084563
20.8	8.055555556	0.001875129	2.728583611	200.927357	3.90626054	4.292381	4.03705272
21.2	8.055555556	0.001875129	2.677100901	204.7913447	3.90626054	4.291994	4.037021781
21.6	8.055555556	0.001875129	2.627524959	208.6553323	3.90626054	4.291618	4.036991706
22	8.055555556	0.001875129	2.579751778	212.5193199	3.90626054	4.291252	4.036962453
22.4	8.055555556	0.001875129	2.533684782	216.3833076	3.90626054	4.290895	4.036933988
22.8	8.0555555	0.0018751	2.4892341	220.24729	3.906260	4.290549	4.0369062

	56	29	71	52	54		75
23.2	8.055555556	0.001875129	2.446316341	224.1112828	3.90626054	4.290211	4.036879281
23.6	8.055555556	0.001875129	2.404853352	227.9752705	3.90626054	4.289881	4.036852976
24	8.055555556	0.001875129	2.364772463	231.8392581	3.90626054	4.28956	4.036827331
24.4	8.055555556	0.001875129	2.326005701	235.7032457	3.90626054	4.289247	4.036802319
24.8	8.055555556	0.001875129	2.28848948	239.5672334	3.90626054	4.288942	4.036777914
25.2	8.055555556	0.001875129	2.252164225	243.431221	3.90626054	4.288644	4.036754093
25.6	8.055555556	0.001875129	2.216974184	247.2952087	3.90626054	4.288353	4.036730832
26	8.055555556	0.001875129	2.182866889	251.1591963	3.90626054	4.288068	4.036708109
26.4	8.055555556	0.001875129	2.149793148	255.0231839	3.90626054	4.287791	4.036685904
26.8	8.055555556	0.001875129	2.117706683	258.8871716	3.90626054	4.287519	4.036664199
27.2	8.055555556	0.001875129	2.086563938	262.7511592	3.90626054	4.287253	4.036642973
27.6	8.055555556	0.001875129	2.056323881	266.6151468	3.90626054	4.286993	4.036622211
28	8.055555556	0.001875129	2.026947825	270.4791345	3.90626054	4.286739	4.036601894
28.4	8.055555556	0.001875129	1.998399264	274.3431221	3.90626054	4.28649	4.036582009
28.8	8.055555556	0.001875129	1.970643719	278.2071097	3.90626054	4.286247	4.036562538
29.2	8.055555556	0.001875129	1.9436486	282.0710974	3.90626054	4.286008	4.03654347
29.6	8.055555556	0.001875129	1.917383078	285.935085	3.90626054	4.285774	4.036524788
30	8.055555556	0.001875129	1.89181797	289.7990726	3.90626054	4.285545	4.036506482
30.4	8.055555556	0.001875129	1.866925628	293.6630603	3.90626054	4.285321	4.036488538
30.8	8.055555556	0.001875129	1.842679841	297.5270479	3.90626054	4.285101	4.036470944